

Cloete, Schalk; Ruhnau, Oliver; Hirth, Lion

Working Paper

On capital utilization in the hydrogen economy: The quest to minimize idle capacity in renewables-rich energy systems

Suggested Citation: Cloete, Schalk; Ruhnau, Oliver; Hirth, Lion (2020) : On capital utilization in the hydrogen economy: The quest to minimize idle capacity in renewables-rich energy systems, ZBW - Leibniz Information Centre for Economics, Kiel, Hamburg

This Version is available at:

<https://hdl.handle.net/10419/222474>

Standard-Nutzungsbedingungen:

Die Dokumente auf EconStor dürfen zu eigenen wissenschaftlichen Zwecken und zum Privatgebrauch gespeichert und kopiert werden.

Sie dürfen die Dokumente nicht für öffentliche oder kommerzielle Zwecke vervielfältigen, öffentlich ausstellen, öffentlich zugänglich machen, vertreiben oder anderweitig nutzen.

Sofern die Verfasser die Dokumente unter Open-Content-Lizenzen (insbesondere CC-Lizenzen) zur Verfügung gestellt haben sollten, gelten abweichend von diesen Nutzungsbedingungen die in der dort genannten Lizenz gewährten Nutzungsrechte.

Terms of use:

Documents in EconStor may be saved and copied for your personal and scholarly purposes.

You are not to copy documents for public or commercial purposes, to exhibit the documents publicly, to make them publicly available on the internet, or to distribute or otherwise use the documents in public.

If the documents have been made available under an Open Content Licence (especially Creative Commons Licences), you may exercise further usage rights as specified in the indicated licence.

On capital utilization in the hydrogen economy: The quest to minimize idle capacity in renewables-rich energy systems

Schalk Cloete^{1}, Oliver Ruhnau², and Lion Hirth^{2,3,4}*

¹ SINTEF Industry, Trondheim, Norway

² Hertie School of Governance, Berlin

³ Neon Neue Energieökonomik GmbH

⁴ Mercator Research Institute on Global Commons and Climate Change (MCC)

*Corresponding author

Flow Technology Group, SINTEF Industry

S.P. Andersens vei 15B, 7031 Trondheim, Norway

Email: schalk.cloete@sintef.no

Abstract

The hydrogen economy is currently experiencing a surge in attention, partly due to the possibility of absorbing wind and solar energy production peaks through electrolysis. A fundamental challenge with this approach is low utilization rates of various parts of the integrated electricity-hydrogen system. To assess the importance of capacity utilization, this paper introduces a novel stylized numerical energy system model incorporating the major elements of electricity and hydrogen generation, transmission and storage, including both "green" hydrogen from electrolysis and "blue" hydrogen from natural gas reforming with CO₂ capture and storage (CCS). Balancing renewables with electrolysis results in low utilization of electrolyzers, hydrogen pipelines and storage infrastructure, or electricity transmission networks, depending on whether electrolyzers are co-located with wind farms or demand centers. Blue hydrogen scenarios face similar constraints. High renewable shares impose low utilization rates of CO₂ capture, transport and storage infrastructure for conventional CCS, and of hydrogen transmission and storage infrastructure for a novel process (gas switching reforming) that enables flexible power and hydrogen production. In conclusion, both green and blue hydrogen can facilitate the integration of wind and solar energy, but the cost related to low capacity utilization erodes much of the expected economic benefit.

Keywords: hydrogen economy; energy system model; decarbonization; CO₂ capture and storage; variable renewable energy.

Nomenclature

Acronyms:

AUSC	Advanced ultra-supercritical coal power plant
CCS	CO ₂ capture and storage
D&I	Distribution and imports
GSR	Gas switching reforming power and hydrogen plant
H2CC	Hydrogen combined cycle power plant
H2GT	Hydrogen open cycle power plant
IEA	International Energy Agency
LCOEH	Levelized cost of electricity and hydrogen
LHV	Lower heating value
NGCC	Natural gas combined cycle power plant
O&M	Operating and maintenance
OCGT	Open cycle gas turbine power plant
PEM	Polymer electrolyte membrane electrolyzer
PV	Photovoltaics
SMR	Steam methane reforming
T&S	Transport and storage
tpa	Tons per annum
VRE	Variable renewable energy

Symbols:

α	Availability (%)
δ	Load (MW)
η	Efficiency (%)
C	Total system cost (€)
c^{fix}	Fixed annual costs (€/MW/year or €/MWh/year)
c^{var}	Variable costs (€/MWh)

d	Energy demand (MW)
e	CO ₂ emissions intensity (kg/MWh)
g	Rate of electricity generation (MW)
g^{H_2}	Rate of hydrogen production (MW)
\hat{g}	Installed generating capacity (MW)
\hat{g}^{H_2}	Installed hydrogen production capacity (MW)
I	Rate of energy imports (MW)
\hat{n}	Installed network capacity (MW)
p	Sales price (€/MWh)
s	Rate of storage (MW)
v	Current level of energy storage (MWh)
\hat{v}	Installed storage volume (MWh)
y	Share (%)

Sub- and superscripts:

bat	Battery
connect	Connectors
i	Index for all technologies generating or consuming electricity
in	Energy in (charging)
j	Index for all storage technologies
k	Index for all network technologies
GSR	GSR electric efficiency (electricity output / fuel input)
GSRH ₂	GSR electric efficiency in hydrogen production mode (electricity output / fuel input)
H ₂ CC	Hydrogen combined cycle plant
H ₂ dist	Hydrogen distribution
H ₂ GSR	GSR hydrogen production efficiency (H ₂ output / fuel input)
H ₂ GT	Hydrogen open cycle plant
H ₂ trans	Hydrogen transmission
H ₂ transalt	Added hydrogen transmission to and from salt caverns
H ₂ transco	Added hydrogen transmission in the wind-electrolysis co-location scenario
NH ₃	Ammonia
out	Energy out (discharging)
PEM	PEM electrolysis
recon	Ammonia reconversion plant
salt	Salt cavern hydrogen storage
SMR	Steam methane reforming with CCS
t	Time (hours)
tank	Tank hydrogen storage
trans	transmission
transolar	Added variable renewable energy transmission for solar
transwind	Added variable renewable energy transmission for wind
v	Battery storage volume
VRE	Variable renewable energy

1 Introduction

Following the Paris Climate Accord established in 2015 [1], climate change has been gradually moving up the political agenda. More recently, the Intergovernmental Panel on Climate Change report on global warming of 1.5 °C [2] has increased urgency by quantifying the unprecedented speed of change needed to avert the worst effects of climate change. As a first major commitment to achieving

decarbonation at a rate close to the scientific consensus, the European Union recently released plans for the European Green Deal [3], striving to become the first climate neutral continent by 2050.

Achieving climate neutrality, not only in the electricity sector, but across the entire economy, is a great economic, technological and societal challenge. One promising pathway to such broad decarbonization that is enjoying a resurgence in attention is the hydrogen economy. Hydrogen has the potential to displace fossil fuel use in transport (fuel cells or synthetic fuels), industry (chemical feedstock, reduction agent or high-grade heat) and buildings (blending in natural gas networks or use in fuel cell combined heat and power plants). In addition, hydrogen from electrolysis run on cheap excess wind and solar electricity could help balance the electricity grid. For these reasons, power-to-gas is increasingly seen as a key component in the future clean energy system [4].

Various high-level reports on hydrogen have been produced over the past two years. The EU hydrogen roadmap states directly that hydrogen is mandatory for deep decarbonization, placing special emphasis on decarbonizing the gas grid, long-distance freight, and high-grade industrial heat [5]. A large consortium of industries in the US also released a hydrogen roadmap, placing emphasis on the economic opportunities of a strong hydrogen industry, highlighting energy security, decarbonization of transport and industry, and electricity system flexibility [6]. The UK strategy sees hydrogen as an important complement to electrification and has a special emphasis on heat, given the UK's large gas grid [7]. In Australia, the emphasis falls on energy security, electricity grid stability and exports [8].

The International Renewable Energy Agency has also produced a report on the connection between hydrogen and renewables [9], highlighting the sector-coupling and balancing benefits that hydrogen offers to variable renewable energy (VRE). Another comprehensive hydrogen report was recently released by the International Energy Agency [10], offering a broad techno-economic overview of many different avenues for hydrogen production, transport, storage and end-use. The report emphasizes that local resources strongly influence the attractiveness of different hydrogen production pathways, requiring regional strategies. For example, electrolysis will be attractive for natural gas importing regions with excellent wind and solar resources, whereas natural gas with CO₂ capture and storage (CCS) is more attractive for natural gas exporters or regions with average wind and solar resources. The challenge of hydrogen's low energy density when dealing with transport and storage is also emphasized, potentially requiring conversion to more practical fuels at considerable additional costs. A wide range of end-uses are also described, along with near-term priorities for kickstarting the hydrogen economy.

One key challenge with hydrogen from VRE is low capacity utilization. Agora Energiewende [11] found 3000-4000 full load hours to be the lower limit for electrolyzers to economically produce synfuels. This means that using electrolyzers only for utilizing occasional wind and solar peaks that would otherwise be spilled is not a viable strategy. Instead, construction of wind and solar facilities dedicated to synfuel production is recommended in certain world regions that can guarantee high electrolyzer utilization rates. This report therefore sees little potential for using electrolysis for balancing higher VRE shares.

Another important aspect that is rarely discussed in the literature is that low electrolyzer utilization rates also impose low utilization of the electricity grid between renewables and electrolyzers, as well as the hydrogen transmission and storage infrastructure necessary for delivering intermittent influxes of hydrogen to consumers. As noted in the IEA report, hydrogen has relatively low energy density, making it substantially more expensive to transport and store than liquid fuels or even natural gas [10].

The optimum between low electricity costs of excess wind and solar and high utilization rates for lower capital costs may therefore lie further towards high capacity utilization than commonly assumed.

The objective of the present study is to explore the role of "green" hydrogen from electrolysis and "blue" hydrogen from natural gas with CCS in a future low-carbon energy system with high shares of VRE. In particular, the implications of intermittency on capital utilization across the entire electricity-hydrogen system are investigated.

This work makes three noteworthy contributions to the literature. First, a novel stylized numerical energy system model for simultaneous optimization of the main elements related to electricity and hydrogen production (10 different power plants, electrolyzers, natural gas reforming with CCS, and clean ammonia imports), distribution (electricity transmission lines and hydrogen pipelines) and storage (batteries, salt cavern storage and tank storage) is developed. Second, the electricity-hydrogen system model is used to deliver new perspectives on the trade-offs involved in variable hydrogen production for utilization of low-cost excess wind and solar power. Third, the potential for low-cost blue hydrogen from advanced CCS processes is considered next to large cost reductions for VRE, electrolyzers and battery storage, quantifying the total system costs and emissions that may be expected from different visions for the hydrogen economy.

The main finding is that capacity utilization imposes an important economic constraint on VRE integration using hydrogen, regardless of the chosen system development pathway. Various solutions can be devised to shift this cost from one part of the energy system to another. For example, when electrolyzers are co-located with wind farms instead of demand centers, the cost of a large electricity grid expansion is displaced by the cost of a large buildout of hydrogen transmission and storage infrastructure supplied by electrolyzers with a low utilization rate. Similarly, a blue hydrogen technology capable of flexible power and hydrogen production increases the utilization of CO₂ capture, transport and storage infrastructure at the expense of hydrogen transport and storage infrastructure. However, blue hydrogen scenarios are less sensitive to the challenge of low capacity utilization because VRE supplies a lower share of total energy, resulting in lower system costs.

The next section reviews some key papers from the field, followed by a description of the modelled energy system in Section 3. Subsequently, the equation system and various technology cost assumptions are outlined in Section 4. Results are presented in Section 5, investigating the impact of total system hydrogen demand, CO₂ pricing and sensitivity to several key model assumptions. The study concludes in Section 6.

2 Literature review

Several studies have been carried out to investigate the potential of the hydrogen economy based on electrolysis from wind and solar power. In addition to the cost and utilization of electrolyzers, cost-effective storage and distribution of hydrogen become very important when using variable wind and solar power. Different storage and distribution options were investigated by Reuß, Grube [12], finding that cavern storage is generally most economical for higher hydrogen demand scenarios, while pipelines are preferred for distribution over longer distances. Liquid organic hydrogen carriers are optimal for storage and distribution at lower hydrogen demand. A detailed spatial modelling study mapped out a hydrogen distribution network for Germany, confirming these findings [13]. For high hydrogen demand scenarios, a combination of cavern storage and pipeline distribution could achieve

hydrogen costs at fuel stations of 6.7-7.5 €/kg. Electrolyzer utilization was about 50%, which is sufficient according to the aforementioned Agora Energiewende report [11]. By focusing only on passenger cars, however, the maximum hydrogen production in this study was only 96 TWh/year – about 5% of total German oil and gas consumption outside of the electricity sector [11].

In the study by Emonts, Reuß [13], the power system was exogenously specified. In contrast, Welder, Ryberg [14] investigate renewable hydrogen supply using concurrently optimized deployment of wind turbines, electrolyzers, storage and transmission. This dedicated hydrogen generation system was designed independently of the power system, satisfying hydrogen demand about 50% higher than in Emonts, Reuß [13] due to inclusion of additional industrial demand. For different hydrogen demand scenarios, production costs of around €7.8/kg were found when adding costs for hydrogen distribution and fuel stations. If salt cavern storage is not available, the hydrogen cost increased by €1.5/kg because the low energy density of hydrogen makes storage in dedicated vessels relatively expensive.

To give some perspective on the economic challenges faced by such green hydrogen scenarios, it can be mentioned that gasoline produced from €50/barrel oil subject to a €100/ton CO₂ tax and reasonable refinement and distribution costs derived from EIA [14] amounts to an equivalent cost of only €2.85/kg hydrogen. This cost gap will increase further when displacing direct use of oil and gas in industry.

A modelling study focused on the UK [15] investigated renewable hydrogen from wind power for decarbonizing transport and found that such an objective is technically feasible using onshore wind power only. Direct hydrogen production costs were not provided, but some valuable insights about the cost implications of various non-idealities in the system are given. If underground storage is not available, the system costs increased by 25%, similar to the finding of Welder, Ryberg [16]. An 11% cost increase is observed when hydrogen transmission pipelines are not permitted and high voltage alternating current transmission lines must be used instead. If these transmission lines must be installed underground, a large additional cost increase of 37% is observed.

System benefits can also be derived by using hydrogen in other sectors. For example, produced hydrogen can be injected into existing natural gas networks to circumvent additional storage and distribution costs, bringing significant system benefits [17]. However, the scale of this strategy is limited by permitted hydrogen blending ratios. Produced hydrogen can also be converted back to power when demand is high. However, when power-to-gas is deployed as an electricity storage medium in this way, it becomes less attractive than pumped hydro storage [18], largely due to the low round-trip efficiency. This may still be an alternative for deep decarbonization in regions without access to pumped hydro storage.

A comprehensive study by Brown, Schlachtberger [19] investigated scenarios for electricity, road transport and heat in a European energy system that is 95% decarbonized via renewables. Hydrogen was included as a source of flexibility for the electricity system, but the demand for hydrogen decreased with increasing system coupling and electricity grid interconnection. However, the study did not consider the potential for cheap salt cavern storage, the possibility of hydrogen pipelines to substitute for electricity grid expansion, and potential hydrogen demand from industry and long-distance transport modes. Hence, the role of hydrogen in optimized clean energy systems may be significantly larger than suggested by this study.

The contribution of hydrogen to the future energy system can also be increased by considering not only "green" hydrogen from renewables but also "blue" hydrogen from fossil fuels with CCS. Blue hydrogen technologies can produce a steady hydrogen output and change output according to demand, avoiding the capacity utilization challenges related to intermittent hydrogen production from excess VRE. The IEA found blue hydrogen to be generally competitive with green hydrogen in the long term, when considering production costs only [10]. However, the IEA report made no provision for next-generation blue hydrogen technologies with the potential to greatly reduce hydrogen production costs, even below the costs of current steam methane reforming without CCS [20, 21]. Our previous study [22] showed that one such technology, gas switching reforming [23], can significantly reduce future energy system costs and emissions by offering flexible power and hydrogen production from natural gas [24].

3 The modelled system

This work extends the scope of our previous study [22] to more comprehensively reflect the full system costs of a renewables-based power system relying on hydrogen for a large degree of flexibility. The modelled system is summarized in Figure 1, illustrating the connections between producers, consumers and storage of electricity and hydrogen.

The following technologies are considered, all of which are assumed to be deployed as large-scale, centralized plants:

- For electricity generation, ten different technologies are considered: wind power, solar PV, pulverized coal and natural gas combined cycle plants with and without CCS, open cycle gas turbines, hydrogen combined and open cycle plants, and gas switching reforming (GSR) [22].
- Lithium ion batteries can be deployed for electricity storage.
- Hydrogen can be produced using three low- or zero-emission technologies: GSR, steam methane reforming (SMR) with CCS, and polymer electrolyte membrane (PEM) electrolysis. No provision is made for "grey" hydrogen production from fossil fuels without CCS.
- Fluctuations in hydrogen production (demand is constant) can be buffered by two storage technologies, cheap salt caverns with slow charge and discharge rates and more expensive storage tanks without any charge/discharge rate limits.
- Hydrogen demand can also be fulfilled with imported clean ammonia that is reconverted to hydrogen in reconversion plants included in the model.

In addition to the flexible electricity demand from electrolysis and batteries, a fixed load profile is imposed based on historical data. Swings in the electricity system stemming from fluctuating load and renewable energy supply can be balanced using dispatchable power plants, electricity generation or minor electricity consumption from GSR, electricity consumption from electrolysis, or battery storage.

Two energy system design philosophies are investigated: a case where electrolyzers are located close to demand centers (Figure 1) and another case where electrolyzers are co-located with wind generators (Figure 2). In the following, the investment and dispatch is optimized for each of these cases, and the results are contrasted to draw conclusions on the different design philosophies.

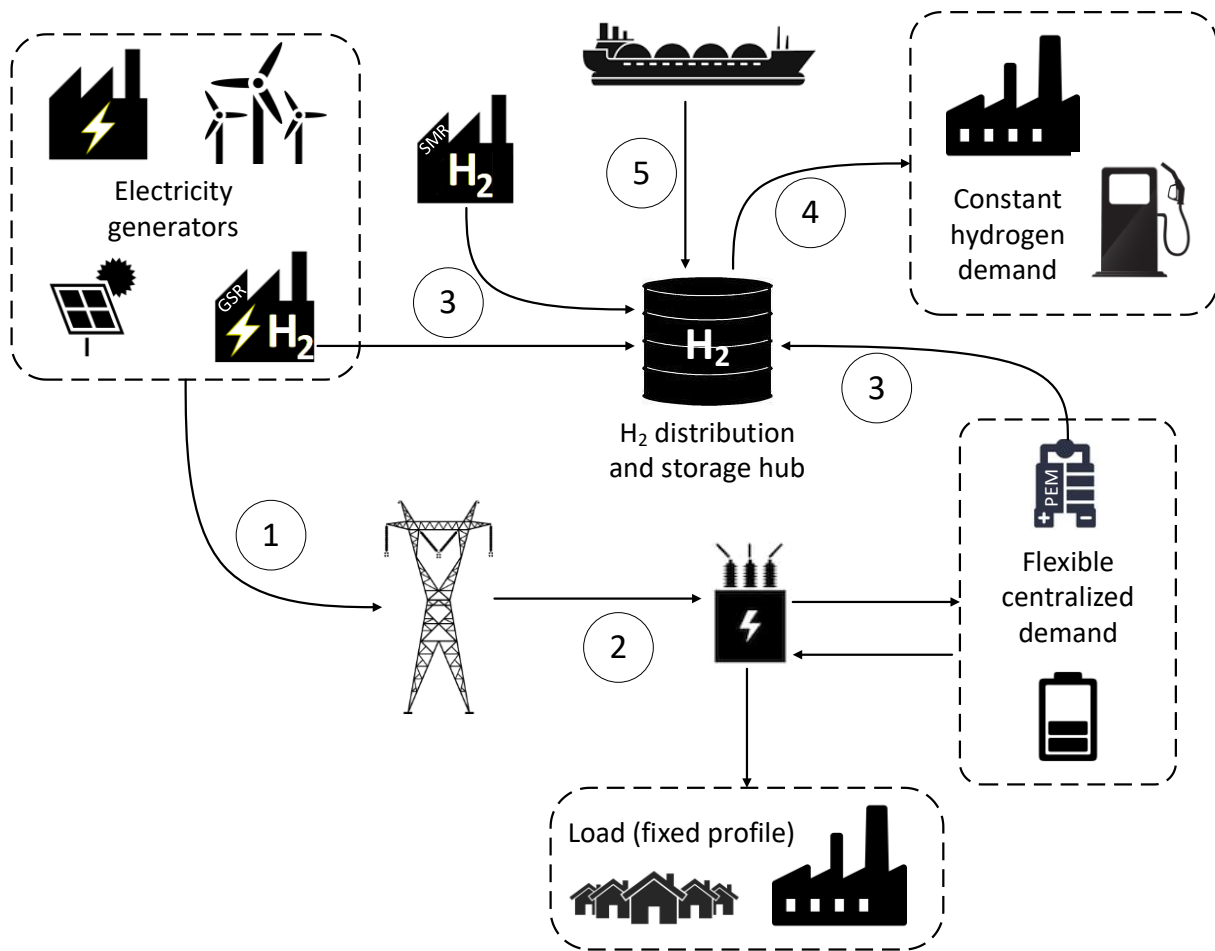


Figure 1: Graphical summary of the modelled system with electrolysis-demand co-location. The numbers represent the following costs: 1) additional transmission costs for wind and solar; 2) conventional transmission costs; 3) hydrogen transmission; 4) hydrogen distribution; 5) reconversion of imported NH_3 .

Important transmission and distribution costs are indicated by numbers on Figure 1 for the case with electrolysis-demand co-location. First, to justify the assumption of copperplate transmission, an additional transmission cost is added to wind and solar power (1) since these technologies are often constructed far from demand centers in regions with high resource quality and low public resistance. This cost is expressed per unit generating capacity of wind and solar power. The next important cost is that of the general electricity transmission network (2), which is calculated proportionally to the maximum total load on the network (the fixed load profile plus demand from centralized electrolysis and batteries) over all hours in the simulated year. Next, the cost of high-pressure hydrogen transmission from centralized production plants to more decentralized hydrogen distribution and storage hubs is included (3), proportionally to the maximum production capacity of hydrogen production plants. Additional hydrogen transmission costs are also added for salt cavern storage because it is only available in certain regions. The cost of more expensive hydrogen distribution pipelines to end-users is also added (4), proportionately to the constant hydrogen demand. Finally, provision is also made for international hydrogen imports in the form of ammonia. In addition to the import cost, the cost and energy penalty of reconverting ammonia back to hydrogen is added in the model (5) with the resulting hydrogen being distributed or stored. No potential for exports is considered as Europe with its relatively poor solar resource, high natural gas prices and high labor costs would not be able to compete in an international clean hydrogen market.

An additional scenario where electrolysis capacity is co-located with wind power close to cheap salt cavern storage is also considered in the study. This is the hydrogen vision generally considered for Germany [13, 25], given the good wind resources concentrated in the north of the country where large salt cavern storage is also available. It is therefore considered only for green hydrogen in this work. Such wind-electrolyzer co-location avoids the electricity transmission network costs involved in transmitting electricity to electrolyzers co-located with demand centers as assumed in Figure 1. The trade-off is that electrolyzers installed in the north do not have access to solar power mostly installed in the south, and that hydrogen needs to be transmitted from a distant production region throughout the country.

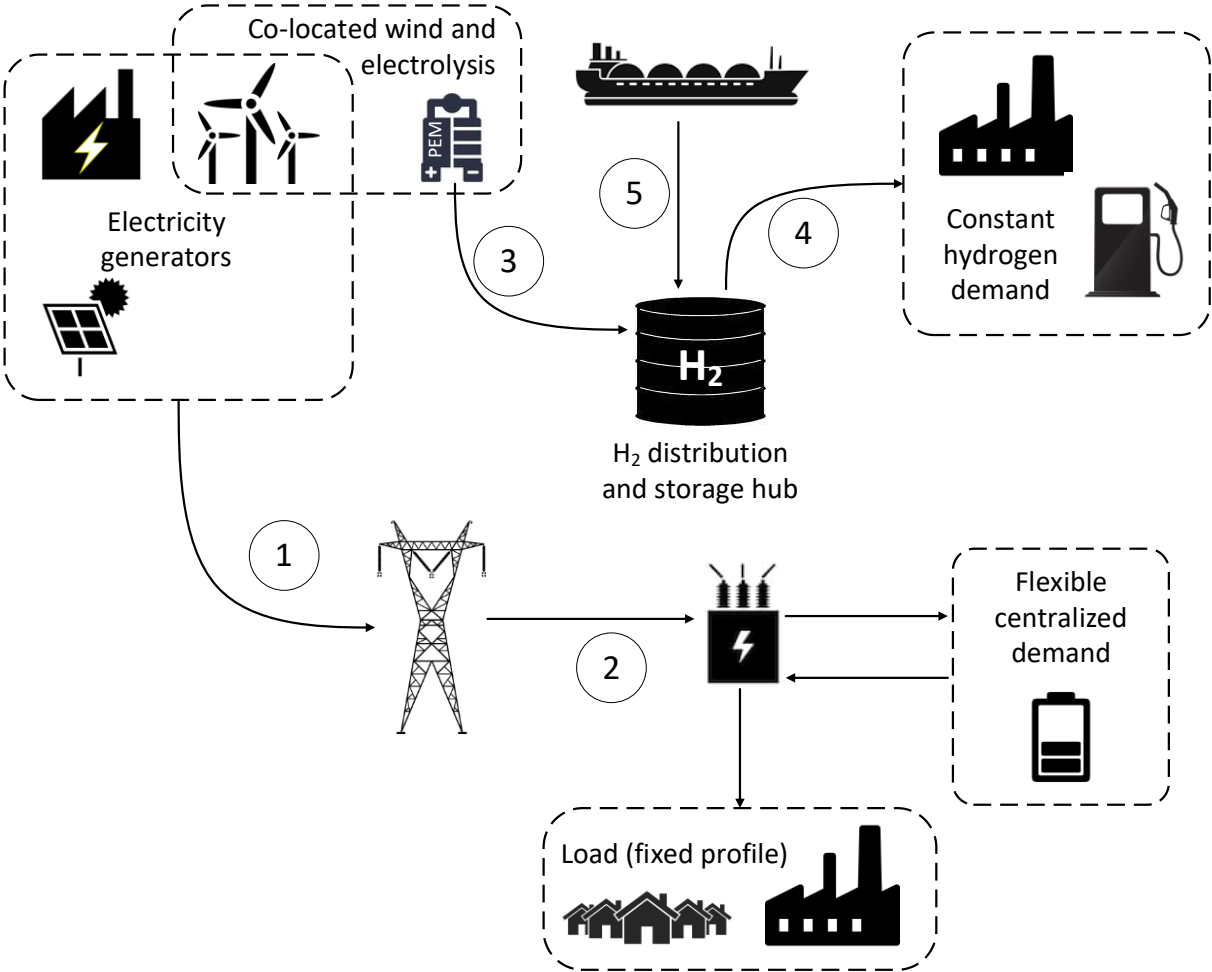


Figure 2: Graphical summary of the modelled system in the wind-electrolysis co-location scenario. The numbers are the same as in Figure 1.

Figure 2 illustrates this scenario. Important differences with the scenarios illustrated in Figure 1 can be highlighted here. First, co-locating wind and electrolysis lowers added VRE transmission costs (1). Electrolysis capacity is subtracted from wind capacity when this cost is calculated. Second, electrolysis does not increase general electricity transmission costs (2) as was the case in Figure 1. Third, added hydrogen transmission costs to cheap salt cavern storage (3) is removed on the assumption that salt caverns are close to the co-located wind farms and electrolyzers. Fourth, hydrogen transmission costs are added to the hydrogen distribution costs calculated proportionately to hydrogen demand (4) to

account for the longer distance over which hydrogen must be transported when electrolysis is co-located with wind generators instead of demand centers.

The objective of the model is to optimize investment in all these generation, transmission, distribution, conversion, storage and end-use technologies to minimize total system cost.

4 Methodology

The methodology is presented in four sections: 1) the model framework used for the system-scale assessment, 2) technology cost assumptions, 3) the main system-scale performance metrics, and 4) a description of the four scenarios considered.

4.1 Model framework

The model considers one representative year and hourly granularity of plant dispatch. Wind, solar and load data are derived from historical German observations, with no cross-border trade. Technology costs applicable to Europe in the year 2040 are used in annualized terms. A long-term view is taken, implying that the model optimizes the technology mix without considering existing infrastructure (“green field” approach) and without constraints on installed capacity.

The objective of the model is to minimize total system costs depicted in Equation 1 by optimizing the deployed capacity of electricity generators and centralized consumers (\hat{g}), electricity and hydrogen storage (\hat{v}) and transmission and distribution networks (\hat{n}), as well as hourly power production (g) from each generating technology, SMR-CCS capacity ($\hat{g}_{\text{SMR}}^{\text{H}_2}$) and hourly hydrogen production ($g_{\text{SMR}}^{\text{H}_2}$), and hourly ammonia imports (I_{NH_3}). From left to right, the terms on the right hand side represent: annualized capital costs and fixed operating and maintenance (O&M) costs for electricity generators (i), storage volume (j) and network capacity (k); fuel, CO₂ and other variable O&M costs summed over all relevant generating technologies and all hours of the year (t); fixed and variable costs for SMR-CCS plants; and the cost of imported ammonia at a specified import price (p_{NH_3}). Section 4.2 details the assumptions regarding fixed (c^{fix}) and variable (c^{var}) costs for each technology.

$$C = \sum_i c_i^{\text{fix}} \hat{g}_i + \sum_j c_j^{\text{fix}} \hat{v}_j + \sum_k c_k^{\text{fix}} \hat{n}_k + \sum_{t,i} c_i^{\text{var}} g_{t,i} + c_{\text{SMR}}^{\text{fix}} \hat{g}_{\text{SMR}}^{\text{H}_2} + \sum_t c_{\text{SMR}}^{\text{var}} g_{t,\text{SMR}}^{\text{H}_2} + \sum_t I_{t,\text{NH}_3} p_{\text{NH}_3} \quad \text{Equation 1}$$

Numerous additional constraints are imposed to define the modelled system. In the following paragraphs, these constraints are presented for the demand-electrolysis co-location scenario (Figure 1), after which the modifications for the wind-electrolysis co-location scenario (Figure 2) are outlined.

The overall electricity balance (Equation 2) states that load must equal the sum of all forms of electricity generation and consumption (negative generation) in the system for every hour of the year. The load profile was taken for Germany for the year 2012 from the Open Power System Data project [26]. Electricity generation includes power production from all generating technologies as well as battery discharge, whereas electricity consumption includes PEM, battery charging, GSR operating in H₂ mode, and reconversion plants for imported ammonia.

$$\delta_t = \sum_i g_{t,i} \quad \forall t \quad \text{Equation 2}$$

For electricity generating technologies, hourly generation is constrained to the maximum available (α) capacity for every hour of the year. For dispatchable generators $\alpha = 1$, whereas maximum availability profiles for wind and solar are adjusted from 2012 data for Germany from the Open Power System Data project [26] to correctly reflect improved technology performance in Europe in the year 2040, resulting in an annual capacity factors of 30% for wind and 14% for solar [27].

$$g_{t,i} \leq \alpha_{t,i} \hat{g}_i \quad \forall t, i \quad \text{Equation 3}$$

The full year capacity factor of any generating technology cannot exceed 0.9 to reflect the need for plant downtime for routine maintenance, based on data from the National Renewable Energy Laboratory [28]. This constraint is slightly modified for the GSR technology to accurately reflect that the combined capacity factor of power and hydrogen production cannot exceed 0.9 [22].

$$\sum_t g_{t,i} \leq 0.9 \cdot 8760 \cdot \hat{g}_i \quad \forall i \quad \text{Equation 4}$$

Hourly power consumption or generation from PEM and batteries is constrained to the installed capacities of these technologies (\hat{g}_{PEM} and \hat{g}_{bat}) in Equation 5 - Equation 7. In addition, imported ammonia reconversion plants also consume power equivalent to 1.25% of the lower heating value (LHV) of imported ammonia [10] (Equation 8). It is important to note that generation from PEM (g_{PEM}), battery charging ($g_{\text{bat}}^{\text{in}}$), and ammonia reconversion plants (g_{recon}) are negative. It is also noted that, unlike all other generating capacity, which is expressed in MW electric, \hat{g}_{recon} in MW ammonia (LHV).

$$-g_{t,\text{PEM}} \leq \hat{g}_{\text{PEM}} \quad \forall t \quad \text{Equation 5}$$

$$-g_{t,\text{bat}}^{\text{in}} \leq \hat{g}_{\text{bat}} \quad \forall t \quad \text{Equation 6}$$

$$\frac{g_{t,\text{bat}}^{\text{out}}}{\eta_{\text{bat}}} \leq \hat{g}_{\text{bat}} \quad \forall t \quad \text{Equation 7}$$

$$-g_{t,\text{recon}} = 0.0125 \cdot \hat{g}_{\text{recon}} \quad \forall t \quad \text{Equation 8}$$

For batteries, the installed storage volume is another important constraint, where the total volume of stored electricity (v^{el}) cannot exceed the installed energy storage capacity (\hat{v}^{el}). These constraints are shown in Equation 9 and Equation 10, where η_{bat} is the battery charge-discharge efficiency.

$$v_t^{\text{el}} = v_{t-1}^{\text{el}} - \left(g_t^{\text{in}} + \frac{g_t^{\text{out}}}{\eta_{\text{bat}}} \right) \quad \forall t \quad \text{Equation 9}$$

$$v_t^{\text{el}} \leq \hat{v}^{\text{el}} \quad \forall t \quad \text{Equation 10}$$

As for electricity, a global energy balance is also imposed on hydrogen. Equation 11 states that, in all hours of the year, fixed hydrogen demand must equal production from GSR, SMR-CCS and PEM, hydrogen imports after reconversion of ammonia at a given efficiency (η_{NH_3}), net hydrogen withdrawals from storage (positive for withdrawing and negative for adding to stored reserves), and negative production of hydrogen by hydrogen-fired combined and open cycle power plants. Several different levels of hydrogen demand will be investigated in this study. It is noted that g_{GSRH_2} , η_{GSRH_2} and g_{PEM} are negative (both GSR and PEM consume electricity when generating hydrogen)¹. The standard constraints on maximum hourly (Equation 12) and annual (Equation 13) production are also imposed on SMR-CCS plants.

$$d_{\text{H}_2} = g_{t,\text{GSRH}_2} \frac{\eta_{\text{H}_2\text{GSR}}}{\eta_{\text{GSRH}_2}} + g_{t,\text{SMR}}^{\text{H}_2} - g_{t,\text{PEM}} \eta_{\text{PEM}} + I_{t,\text{NH}_3} \eta_{\text{NH}_3} + s_{t,\text{H}_2} - \left(\frac{g_{t,\text{H}_2\text{CC}}}{\eta_{\text{H}_2\text{CC}}} + \frac{g_{t,\text{H}_2\text{GT}}}{\eta_{\text{H}_2\text{GT}}} \right) \quad \forall t \quad \text{Equation 11}$$

$$g_{t,\text{SMR}}^{\text{H}_2} \leq \hat{g}_{\text{SMR}}^{\text{H}_2} \quad \forall t \quad \text{Equation 12}$$

$$\sum_t g_{t,\text{SMR}}^{\text{H}_2} \leq 0.9 \cdot 8760 \cdot \hat{g}_{\text{SMR}}^{\text{H}_2} \quad \text{Equation 13}$$

Hydrogen storage is constrained similarly to battery storage. The evolution of stored hydrogen summed over the two different hydrogen storage technologies is shown in Equation 14, where the final term represents the net rate of hydrogen production from storage introduced in Equation 11. The maximum storage volume of tank hydrogen storage is constrained by its installed capacity (Equation 15), whereas it is set to half the installed capacity for salt cavern storage (Equation 16) because it can only be safely operated between 30% and 80% capacity [29]. An additional constraint is imposed on salt caverns: the storage volume cannot be changed by more than 10% per day [29] (Equation 17).

$$\sum_j v_{t,j}^{\text{H}_2} = \sum_j v_{t-1,j}^{\text{H}_2} - s_{t,\text{H}_2} \quad \forall t \quad \text{Equation 14}$$

$$v_{t,\text{tank}}^{\text{H}_2} \leq \hat{v}_{\text{tank}}^{\text{H}_2} \quad \forall t \quad \text{Equation 15}$$

$$v_{t,\text{salt}}^{\text{H}_2} \leq 0.5 \cdot \hat{v}_{\text{salt}}^{\text{H}_2} \quad \forall t \quad \text{Equation 16}$$

$$\text{abs}(v_{t,\text{salt}}^{\text{H}_2} - v_{t-1}^{\text{H}_2}) \leq \frac{0.1 \cdot \hat{v}_{\text{salt}}^{\text{H}_2}}{24} \quad \forall t \quad \text{Equation 17}$$

Lastly, several constraints are imposed to define electricity transmission as well as hydrogen transmission and distribution. Electricity transmission capacity is sized by the maximum load on the

¹ When GSR operates in hydrogen production mode, $\eta_{\text{H}_2\text{GSR}}$ and η_{GSRH_2} denote the hydrogen and electricity output per quantity of natural gas input, respectively. Thus, $\eta_{\text{H}_2\text{GSR}}/\eta_{\text{GSRH}_2}$ indicates the ratio of hydrogen to electricity output.

network over all hours of the year (Equation 18). This creates an incentive for PEM to run during off-peak hours and for battery charge and discharge to be scheduled for lowering peak system load. Additional transmission capacity is also considered for wind and solar resources given that they are generally constructed further from demand centers than dispatchable generators and may require local grid upgrades to utilize production peaks (Equation 19 and Equation 20).

$$\hat{n}_{\text{trans}} \geq \delta_t - g_{t,\text{PEM}} - g_{t,\text{recon}} - g_{t,\text{bat}}^{\text{in}} - g_{t,\text{bat}}^{\text{out}} \quad \forall t \quad \text{Equation 18}$$

$$\hat{n}_{\text{transwind}} = \hat{g}_{\text{wind}} \quad \text{Equation 19}$$

$$\hat{n}_{\text{transsolar}} = \hat{g}_{\text{solar}} \quad \text{Equation 20}$$

Hydrogen transmission capacity is sized according to the production capacity of GSR, SMR-CCS and PEM technologies (Equation 21), added hydrogen transmission for salt cavern storage is sized for the maximum rate of charge/discharge of salt caverns (Equation 22), and hydrogen distribution capacity is set equal to demand (Equation 23). Finally, Equation 24 states that hydrogen reconversion capacity is sized for peak ammonia import rate.

$$\hat{n}_{\text{H}_2\text{trans}} = \hat{g}_{\text{GSRH}_2} \frac{\eta_{\text{H}_2\text{GSR}}}{\eta_{\text{GSR}}} + \hat{g}_{\text{SMR}} + \hat{g}_{\text{PEM}} \eta_{\text{PEM}} \quad \forall t \quad \text{Equation 21}$$

$$\hat{n}_{\text{H}_2\text{transalt}} = \frac{0.1 \cdot \hat{v}_{\text{salt}}^{\text{H}_2}}{24} \quad \text{Equation 22}$$

$$\hat{n}_{\text{H}_2\text{dist}} = d_{\text{H}_2} \quad \text{Equation 23}$$

$$\hat{n}_{\text{recon}} \geq I_{t,\text{NH}_3} \quad \forall t \quad \text{Equation 24}$$

The wind-electrolysis co-location scenario described in Figure 2 requires some modifications to the equation system given above. First, the required transmission capacity is reduced by replacing Equation 18 with Equation 25 and Equation 19 with Equation 26. These equations state that electrolysis no longer requires transmission network expansion and reduces the added network expansion needed to supply wind power to demand centers. In Equation 26, it is assumed that the connection of electrolysis to several local wind farms to allow access to the smooth country-wide wind profile used in this study requires only a quarter of the usual added wind transmission cost.

$$\hat{n}_{\text{trans}} \geq \delta_t - g_{t,\text{recon}} - g_{t,\text{bat}}^{\text{in}} - g_{t,\text{bat}}^{\text{out}} \quad \forall t \quad \text{Equation 25}$$

$$\hat{n}_{\text{transwind}} = \hat{g}_{\text{wind}} - 0.75 \cdot \hat{g}_{\text{PEM}} \quad \text{Equation 26}$$

On the assumption that the co-located wind and electrolysis plants are also located close to salt cavern storage, the added hydrogen transmission pipelines to remote salt caverns (Equation 22) are removed.

However, an additional hydrogen transmission cost is added for transmitting a steady supply of hydrogen from the concentrated production region throughout the country (Equation 27).

$$\hat{n}_{\text{H}_2\text{transco}} = d_{\text{H}_2} \quad \text{Equation 27}$$

Furthermore, it is assumed that PEM capacity installed in the northern regions close to salt cavern storage does not have access to solar power from the south and a fraction of wind power that is installed too far from salt caverns. Access to these distant VRE resources would require additional grid upgrades that are not considered as an investment option in this scenario. The fraction of wind power installed close enough to salt cavern storage is subject to considerable uncertainty without detailed spatial modelling, which is beyond the scope of this study, but it was approximated here as three quarters of the country-wide wind generation profile. This implies that 75% of the country's wind capacity is installed close enough to salt cavern storage for Equation 22 to be neglected. Thus, electrolysis does not have access to electricity generation from solar and 25% of wind power as shown in Equation 28.

$$-g_{t,\text{PEM}} \leq \sum_i g_{t,i} - 0.25 \cdot g_{t,\text{wind}} - g_{t,\text{solar}} \quad \forall t \quad \text{Equation 28}$$

This system of equations is solved using the General Algebraic Modelling System (GAMS) software to minimize the objective function (Equation 1).

4.2 Technology cost assumptions

This study employs technology cost and performance assumptions consistent with the year 2040. The four sections below outline the assumptions employed regarding capital costs, fuel costs, and O&M costs, adjusted to Euros using a 1.1 \$/€ exchange rate where applicable.

Due to the uncertainty involved in several assumptions, this work includes an extensive sensitivity analysis, which is presented in Section 0.

4.2.1 Capital costs

Wind, solar, coal (AUSC), and gas (NGCC) capital costs are taken from the IEA World Energy Outlook 2019 [27] for Europe in the year 2040. However, due to frequent underestimations of wind and solar cost reductions, the base case in this study assumes an additional 20% cost reduction for wind and solar. The capital cost of open cycle gas turbines (OCGT) is derived from the IEA Projected Costs of Generating Electricity report [30] to be 56% of NGCC plant costs.

For estimating the cost increase of including CCS in coal and gas plants, the European Benchmarking Task Force (EBTF) best practice guidelines [31] are used, resulting in a cost increase of 56% for both coal and gas plants. The cost increase of GSR over a conventional NGCC plant is somewhat larger at 67% [24]. Capital costs related to CO₂ transport and storage are added to the cost of each CCS plant so that the plant will be able to transport and store its peak CO₂ production. These costs were derived from IEA greenhouse gas (IEAGHG) reports [32, 33] as €60/tpa for transport (750 km pipeline) and an additional €35/tpa for storage (aquifer).

The capital costs for SMR-CCS plants, batteries and electrolyzers are taken from the long-term scenario considered by the IEA Future of Hydrogen report [10]. CO₂ T&S costs are added to the SMR-CCS plant cost in the same way as for CCS power plants.

The cost of the electricity transmission network is estimated from German data that the grid contributed about €66/MWh (inflation adjusted) to electricity prices [34] in 2012 (the year selected for load data in the present study). Based on IEA electricity investment projections [27], transmission accounts for only 20% of grid costs, i.e. €13.2/MWh. As another reference point, the most recent grid costs from transmission system operator TenneT is €21.1/MWh [35]. However, this somewhat higher cost may already be influenced by additional costs for VRE integration (which is included separately in this study) and the lower estimate of €13.2/MWh is therefore used. For an annual electricity demand of 515 TWh and peak load of 82 GW based on the load data used in this study, the annualized grid cost amounts to €83/kW/year. Assuming a 7% discount rate, 50-year lifetime and 2% annual O&M costs, the capital cost of all transmission network components amounts to 898 per kW of peak system load.

Added grid-related costs for wind and solar were taken from a review of multiple interconnection studies, actual transmission projects and modelling studies [36]. Cost estimates are spread over a wide range with a mean and median of 506 and 350 \$/kW for wind from 40 reviewed studies and a mean and median of 411 and 266 \$/kW for solar from 15 reviewed studies. Values of €300/kW for wind and €200/kW for solar are assumed here, slightly below the median estimates.

H₂ transmission costs are also uncertain, mainly due to uncertainty in the distance over which hydrogen must be transmitted, especially when it must pass through salt cavern storage that is only available in certain locations. The IEA Future of Hydrogen report [10] estimates the cost of hydrogen pipelines at €0.85/kW/km for GW-scale pipelines and €3.1/kW/km for 100 MW-scale pipelines. Here, the cost is assumed to be €150/kW, equivalent to 48 km of 100 MW-scale pipeline for medium scale plants situated closer to demand centers or 176 km of GW-scale pipeline for large scale plants situated further from demand centers. Additional large-scale hydrogen transmission is implemented for salt cavern storage since these sites are located close to the coast [37], requiring additional transmission to make this cheap storage capacity useful for satisfying inland demand. Given the remote location of these caverns, the cost is set to 200 €/kW for this extra hydrogen transmission capacity, representing an average distance of 235 km to the production facility if GW scale pipelines are used. In the co-location scenario described in Figure 2, additional transmission costs (Equation 27) are estimated from Emonts, Reuß [13] as €650/kW based on costs of about €7 billion for 11 GW of hydrogen demand.

Hydrogen distribution can be done using 100 MW-scale pipelines with small MW-scale lower pressure pipelines branching off to hydrogen fuel stations. These MW-scale pipelines are much more costly at €196/kW/km [10]. Here, an estimate of €500/kW is made on the assumption that the average unit of hydrogen is distributed through 2 km of MW-scale pipeline and 35 km of 100 MW-scale pipeline. This cost is about 30% lower than the cost calculated by Emonts, Reuß [13] only for supplying hydrogen fuel stations on the assumption that there would also be considerable centralized demand from industrial clusters (with lower distribution costs). Ammonia reconversion plant costs are taken from the same source [10]. Hydrogen storage costs are estimated from two reports from Elemental Energy and Argonne Labs [29, 38].

Notable exclusions from the technology mix are biomass, hydropower and pumped storage, nuclear power, and offshore wind. Biomass, hydropower and pumped storage are excluded based on their

limited and widely varying availability across different regions. Nuclear power is excluded due to the large political challenges faced by this technology, especially in Europe. Offshore wind is excluded for simplicity on the assumption that it will see limited deployment next to cheaper onshore wind.

All costs are annualized over the lifetimes indicated in Table 1 using a discount rate of 7%.

Table 1: Capital cost and lifetime assumptions for different technologies.

Technology	Unit	Cost	Lifetime (years)	Reference
Wind	€/kW	1280	25	[27] – 20%
Solar	€/kW	444	30	[27] – 20%
AUSC (coal)	€/kW	1818	40	[27]
NGCC (gas)	€/kW	909	40	[27]
OCGT (gas)	€/kW	509	30	[30]
AUSC-CCS	€/kW	2836	40	[31]
NGCC-CCS	€/kW	1418	40	[31]
GSR (including CO ₂ capture)	€/kW	1518	40	[24]
CO ₂ transport & storage	€/tpa	95	40	[32, 33]
Battery power	€/kW	86	20	[10]
Battery storage	€/kWh	100	20	[10]
Electrolysis	€/kW	409	20	[10]
SMR-CCS	€/kW	1164	40	[10]
Transmission network	€/kW(peak)	898	50	[27, 34]
Wind added transmission	€/kW	300	50	[36]
Solar added transmission	€/kW	200	50	[36]
H ₂ transmission	€/kW	150	25	[10]
H ₂ salt cavern transmission	€/kW	200	25	[10]
H ₂ co-location transmission	€/kW	650	25	[13]
H ₂ distribution	€/kW	500	25	[10]
NH ₃ reconversion	€/kW	520	25	[10]
Salt cavern H ₂ storage	€/kWh	1	25	[29, 38]
Tank H ₂ storage	€/kWh	15	25	[29, 38]

4.2.2 Fuel costs

The fossil fuel costs shown in Table 2 are taken from the Sustainable Development Scenario in the IEA World Energy Outlook for Europe in the year 2040 [27]: 55 €/ton for coal and 6.8 €/MBtu on a gross caloric basis (converted to LHV in this study). The Sustainable Development Scenario is the only IEA scenario with suitable CO₂ prices to match the scenarios considered in the present study.

The price for clean hydrogen imports is based on calculations in the Future of Hydrogen report [10] for hydrogen produced via electrolysis in North Africa, converted to ammonia and exported to Europe to be reconverted to hydrogen and distributed locally. Production, conversion and transmission costs of the ammonia are taken from the report, whereas the reconversion back to hydrogen and local distribution is modeled in this study to correctly reflect the economic benefits of high reconversion plant utilization rates. IEA calculations show that future clean hydrogen imports (excluding reconversion and distribution) in the form of ammonia can cost as little as €25/GJ. However, like fossil fuels, the price importers must pay for internationally traded energy carriers will be much higher than the production cost of the lowest cost exporter. Thus, a value of €35/GJ is assumed.

The possibility to build hydrogen-fired combined (H2CC) and open cycle (H2GT) power plants (assumed to have the same capital costs as NGCC and OCGT plants) is also included. In this case, no fuel cost is specified, but the hydrogen required by these plants is subtracted from the H₂ energy balance (Equation 11), requiring more hydrogen production, transmission, storage and imports to satisfy a given hydrogen demand.

Table 2: Fuel cost and CO₂ intensity assumptions.

Fuel	Base (€/GJ)	CO ₂ intensity (kg/GJ)
Coal	2.2	97
Natural gas	7.1	57
Hydrogen imports	35	-

CO₂ intensities are also provided for fossil fuels (Table 2) in order to calculate the amount of CO₂ that must either be emitted (and paid for under a CO₂ tax) or captured, transported, and stored.

Thermal power plant fuel costs are directly influenced by their net electric efficiency. The efficiency of coal, gas and hydrogen plants are assumed the same as in our previous work [22], based on longer-term potentials of coal [30] and gas [39] plants and CCS energy penalties [24, 31, 40, 41] (Table 3). The round trip efficiency of batteries is taken from the Future of Hydrogen report [10]. Electrolysis efficiency is taken from the same source [10] where long-term efficiencies of 74% are assumed. However, PEM electrolysis typically produces hydrogen at around 20 bar, which is too low for feeding to the transmission network. The GSR plant includes compression power of about 4% of exported hydrogen for compressing hydrogen from 20 bar to 150 bar [24], so this additional penalty is also included for electrolysis, reducing its efficiency to 72%. The Future of Hydrogen report [10] is also the source of SMR-CCS plant efficiency and CO₂ capture assumptions, and the efficiency and electricity consumption of ammonia reconversion to hydrogen.

Table 3: Efficiency and CO₂ capture assumptions for different technologies.

Technology	Efficiency (LHV)	CO ₂ capture
AUSC (coal)	50%	-
NGCC (gas)	65%	-
OCGT (gas)	45%	-
AUSC + CO ₂ capture	41%	90%
NGCC + CO ₂ capture	58%	90%
GSR (power mode)	58%	98%
GSR (H ₂ mode)	84% (H ₂)	98%
	-5% (power)	
Batteries	87%	-
Electrolysis	72%	-
SMR-CCS	69%	90%
NH ₃ reconversion	91% (H ₂)	-
	-1.25% (power)	

4.2.3 Operating and maintenance costs

Table 4 shows the O&M cost assumptions of the different technologies considered in this study. These costs were taken from the same sources as referenced for the capital costs in Table 1.

Table 4: Operating and maintenance cost assumptions for different technologies.

Technology	Fixed (% of CAPEX per year)	Variable (€/MWh)
Wind	2.3	-
Solar	2.2	-
AUSC (coal)	2	3
NGCC (gas)	2.5	2
OCGT (gas)	2.5	2
AUSC + CO ₂ capture	2	5
NGCC + CO ₂ capture	2.5	4
GSR	2.5	4
CO ₂ transport and storage	-	2 €/ton
Battery power	10	-
Battery storage	3	-
Electrolysis	1.5	-
SMR-CCS	3	-
Transmission network	2	-
VRE added transmission	2	-
H ₂ transmission	2	-
H ₂ salt cavern transmission	2	-
H ₂ distribution	2	-
NH ₃ reversion	4	-
Salt cavern H ₂ storage	3	-
Tank H ₂ storage	2	-

4.3 Performance measures

Two main performance measures are used to quantify the system-level performance of each case. First, the system levelized cost of electricity and hydrogen (€/MWh) is defined as the total annual system cost (Equation 1) divided by the total annual electricity and hydrogen supplied to end users. Separating levelized costs for electricity and hydrogen is challenging in an integrated assessment, so, given the similar economic value of these two energy vectors, they are lumped together.

$$LCOEH = \frac{C}{\sum_t \delta_t + d_{H_2} \cdot 8760} \quad \text{Equation 29}$$

Second, the system CO₂ emissions intensity (kg/MWh) is defined in a similar way. All annual CO₂ emissions are summed and divided by the total annual electricity and hydrogen supplied to end users.

$$e_{net} = \frac{\sum_{t,i} e_{i,t} g_{t,i}}{\sum_t \delta_t + d_{H_2} \cdot 8760} \quad \text{Equation 30}$$

In addition, the utilization factor of several types of capital is also defined. For electrolysis, dispatchable power plants (weighted by capital cost), hydrogen transmission and CO₂ T&S, the utilization factor is simply defined as the capacity factor, defined as follows for generic generating technology:

$$CF = \frac{\sum_t g_t}{\hat{g} \cdot 8760}$$

Equation 31

For wind and solar, the utilization factor is defined as the achieved capacity factor divided by the maximum availability: 30% for wind and 14% for solar. This quantifies how much VRE is curtailed.

For transmission capacity, generation in Equation 31 is defined as the total positive electricity generation, and capacity is defined as the total transmission capacity deployed according to Equation 18 or Equation 25. However, for the *CoLoc* scenario, the electricity consumption by PEM is subtracted from the total electricity generation because this electricity is not transmitted through the transmission grid.

4.4 Scenarios

Four scenarios are considered in this study:

- *NoCCS*: All technologies are available except the CCS technologies: AUSC-CCS, NGCC-CCS, SMR-CCS and GSR.
- *CoLoc*: Identical technology availability to the *NoCCS* scenario, except that PEM is co-located with wind close to cheap salt cavern storage (Figure 2 and Equation 25 to Equation 28).
- *CCS*: The “conventional” CCS technologies; AUSC-CCS, NGCC-CCS, SMR-CCS are also made available, but no GSR.
- *AllTech*: All technologies are available.

The *NoCCS* and *CoLoc* scenarios explore the possibility of developing the hydrogen economy based on “green” hydrogen, i.e. hydrogen from wind and solar energy. CCS is assumed to be unavailable, thus automatically excluding “blue” hydrogen from fossil fuels.

Blue hydrogen is made available in the *CCS* and *AllTech* scenarios. The *CCS* scenario includes conventional post combustion CO₂ capture plants applied both to fossil fuel power and hydrogen plants. The *AllTech* scenario also includes the novel GSR technology to investigate its potential to lower system costs and emissions through flexible power and hydrogen production [22].

5 Results and discussion

Results will be presented and discussed in three sections: the performance of the four scenarios under various levels of hydrogen demand, the effect of CO₂ pricing, and the sensitivity of model results to five important parameters.

5.1 Effect of hydrogen demand

Successful establishment of the hydrogen economy opens possibilities for complementary interaction between the power and hydrogen sectors. In green hydrogen scenarios, electrolysis can be deployed to balance VRE, whereas GSR can balance VRE with blue hydrogen. To study this interaction, the optimal technology mixes are calculated in the four scenarios described in Section 4.4 as the hydrogen demand is varied from zero to 600 TWh/year. This hydrogen demand range corresponds to 0-33% of the German total energetic oil and gas consumption in transport, industry and heat in 2015 [11].

The optimal electricity generation mix and CO₂ emissions are shown in Figure 3, employing a CO₂ price of €100/ton. Large increases in electricity generation with hydrogen demand are observed in the green hydrogen scenarios (*NoCCS* and *CoLoc*) where PEM supplies almost all hydrogen. CO₂ emissions intensity remains relatively high due to the large amount of power production from unabated NGCC plants. In the *NoCCS* scenario, the VRE share stays almost constant as hydrogen demand increases, indicating a lack of synergy between VRE and electrolysis. As will be discussed in more detail later, this is due to high transmission system costs that incentivize a high PEM capacity factor. The *CoLoc* scenario circumvents this constraint by co-locating wind and PEM to remove the need for costly transmission capacity to transport electricity from wind farms to electrolyzers. As a result, the optimal VRE share increases from 51% to 60% when hydrogen demand is increased from 0 to 400 TWh/year. However, the VRE share drops down to 55% in the 600 TWh/year hydrogen demand scenario. In this case, total hydrogen demand exceeds electricity demand (515 TWh/year), reducing the potential for synergy between hydrogen and power production.

For the blue hydrogen scenarios (*CCS* and *AllTech*), Figure 3 shows that no electrolysis is deployed in the optimal technology mix. All hydrogen demand is satisfied by SMR-CCS in the *CCS* scenario and GSR in the *AllTech* scenario. Electricity generation in the *CCS* scenario is unaffected by hydrogen demand because SMR-CCS plants are operated independently from the power system. On the other hand, some interaction between power and hydrogen production is visible in the *AllTech* scenario, where the presence of hydrogen demand allows GSR plants to operate as flexible power and hydrogen producers, integrating significantly higher VRE shares. However, the positive effect is smaller than that observed in our previous study [22] with most power production shifting to NGCC-CCS plants. This allows GSR plants to produce a steadier hydrogen output, lowering the cost associated with oversized hydrogen transmission and storage to handle the intermittent hydrogen production profile when GSR is used to balance VRE. CO₂ emissions in the two blue hydrogen scenarios are low due to the low levels of unabated power generation in these scenarios. The *AllTech* scenario further reduces emissions due to the high CO₂ avoidance of GSR.

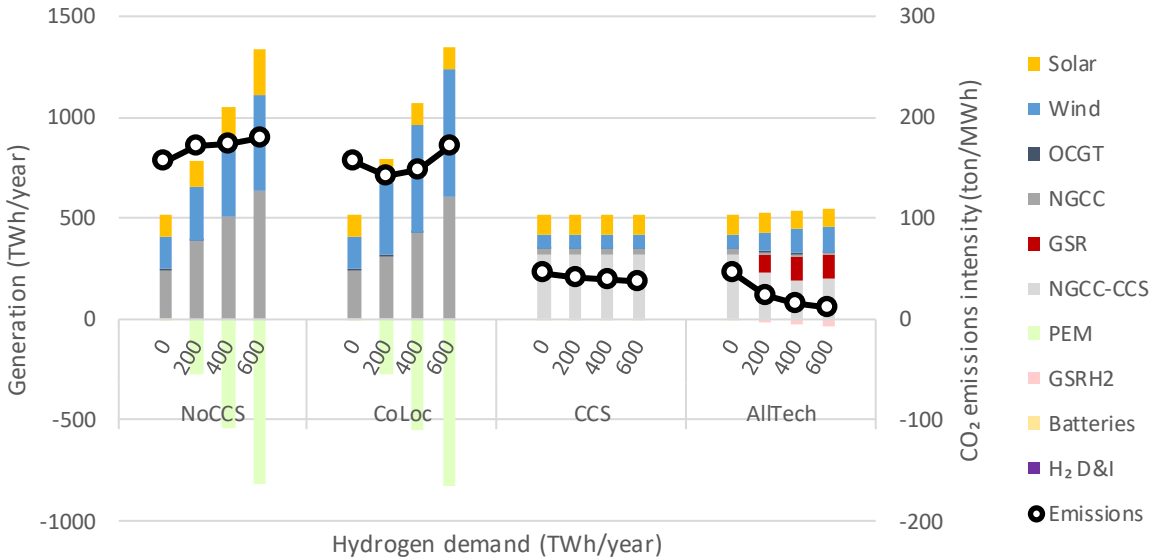


Figure 3: The optimal generation mix and associated CO₂ emissions in the four different scenarios at four different levels of total hydrogen demand. The CO₂ price is set to €100/ton.

Figure 4 shows the total system costs involved in the four scenarios. The most important observation is that the LCOEH (Equation 29) increases with hydrogen demand in the green hydrogen scenarios and decreases in the blue hydrogen scenarios. This is because hydrogen from electricity would always be more expensive than the electricity used to produce it, while fossil fuels can be converted to hydrogen considerably more efficiently than they can be converted to electricity. It is also clear that "other" energy system costs are much higher in the green hydrogen scenarios than the blue hydrogen scenarios.

It should also be mentioned that the green hydrogen scenarios are not completely green because a substantial fraction of the hydrogen is generated using electricity from unabated NGCC plants. The cost increase from imposing strictly green hydrogen was briefly investigated by imposing a limit (via Equation 28) that the hourly PEM consumption cannot exceed combined wind and solar generation in the *NoCCS* scenario and 75% of wind generation in the *CoLoc* scenario. For the case with 400 TWh/year of hydrogen demand, the LCOEH increases from 107 to 110 €/MWh in the *NoCCS* scenario and from 103 to 108 €/MWh in the *CoLoc* scenario. Supplying strictly green hydrogen is therefore not exceedingly expensive. In addition, this constraint forces the system to deploy PEM more as a balancing mechanism for VRE, causing substantial reductions in CO₂ emissions from 173 to 124 kg/MWh in the *NoCCS* scenario and 148 to 73 kg/MWh in the *CoLoc* scenario.

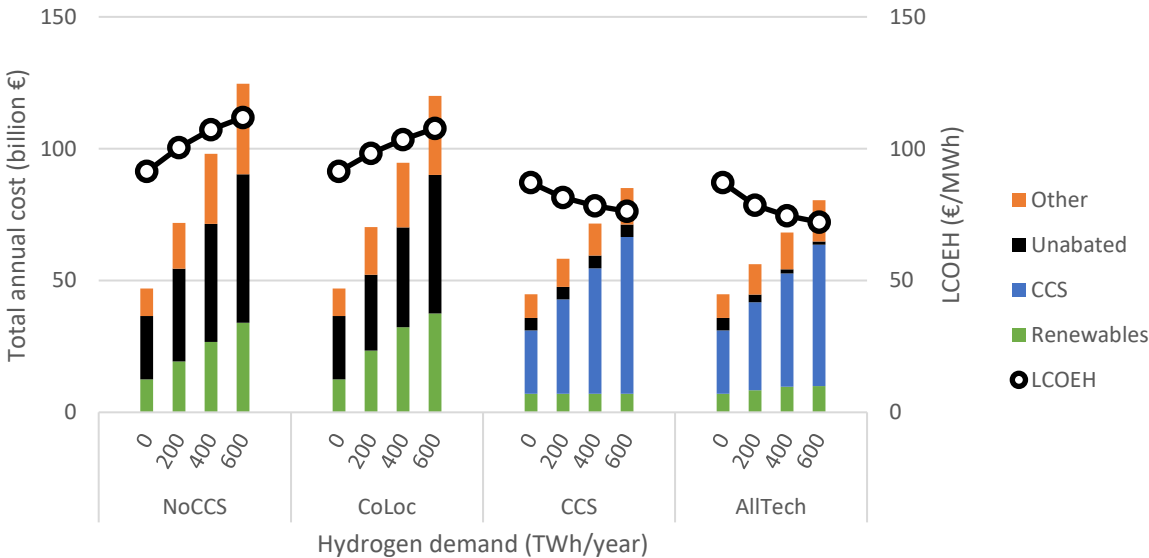


Figure 4: Costs involved in the four different scenarios at four different levels of hydrogen demand. The CO₂ price is set to €100/ton.

A more detailed breakdown of "other" costs in Figure 4 is shown in Figure 5. In the *NoCCS* scenario, electricity transmission accounts for the bulk of the additional system costs due to the need to transmit more power from windy and sunny regions to electrolyzers distributed across the country close to demand centers. The *CoLoc* scenario shows a different trend. In this case, transmission costs remain modest as the co-located PEM capacity minimizes the cost of electricity transmission from wind farms. However, electrolyzer costs are considerably higher as these are operated at a lower capacity factor. Hydrogen transmission and storage costs also increase because hydrogen must be transmitted from

concentrated production in one region to the entire country and more seasonal storage is needed. A small amount of ammonia imports is observed in the *NoCCS* scenario. Overall, the *CoLoc* scenario is slightly cheaper than the *NoCCS* scenario, indicating the lower cost of hydrogen transmission relative to electricity transmission, similar to the finding of Samsatli, Staffell [15].

Figure 5 shows that other costs in the blue hydrogen scenarios remain small. Aside from electricity transmission costs, these costs are limited mainly to hydrogen transmission in the *CCS* scenario and hydrogen transmission and storage in the *AllTech* scenario. Despite GSR operating mainly as a hydrogen plant to reduce the intermittency of hydrogen production, hydrogen handling costs in the *AllTech* scenario are noticeably higher than in the *CCS* scenario due to the lower utilization rate of hydrogen transmission pipelines and the need for hydrogen storage facilities. This is the main factor limiting the flexibility benefit of GSR relative to our previous work [22].

A small amount of battery deployment is also visible in all cases except for the *AllTech* scenario with hydrogen demand where the flexibility offered by GSR displaces battery capacity. This relatively low deployment occurred even though batteries can have an important additional benefit in terms of transmission network cost reduction (Equation 18). Greater battery deployment could be expected in regions with better solar resources where required energy storage timescales are shorter.

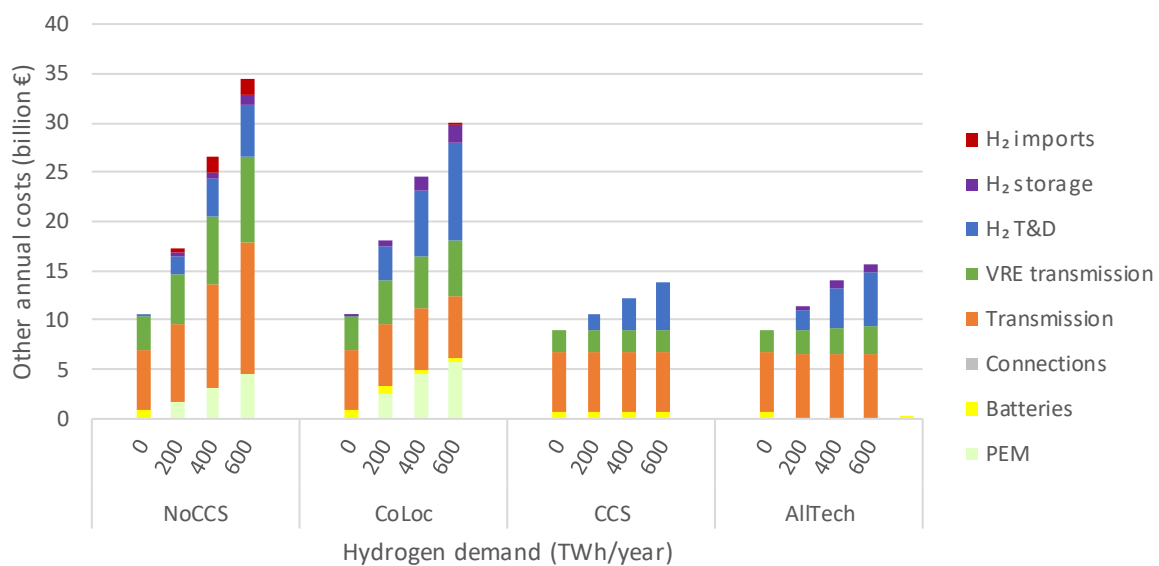


Figure 5: Breakdown of costs other than electricity or hydrogen production ("other" in Figure 4).

Figure 6 displays the capacity utilization factors for different types of capital (defined in Section 4.3) in each of the scenarios. In the *NoCCS* scenario, PEM generates hydrogen at a high capacity factor, also allowing for a high utilization of H₂ transmission infrastructure. Dispatchable plants (mainly NGCC) also enjoy a moderately high utilization rate. Steady operation is the optimal solution in this scenario due to the high cost of electricity transmission needed to supply the large amount of additional electricity (160% more than original electricity demand in the 600 TWh/year hydrogen demand case) to electrolyzers located close to demand centres. Figure 6 shows that the model strategically dispatches PEM and batteries to minimize the required grid capacity in this scenario (Equation 18). PEM plays the greatest role, increasing grid utilization from 77% in the case without hydrogen demand to 90-91% in the cases with hydrogen demand. The grid capacity avoidance benefit of batteries can be seen in the

case without hydrogen demand where peak system load is 81.8 GW, but only 76.8 GW of grid capacity was deployed by the model.

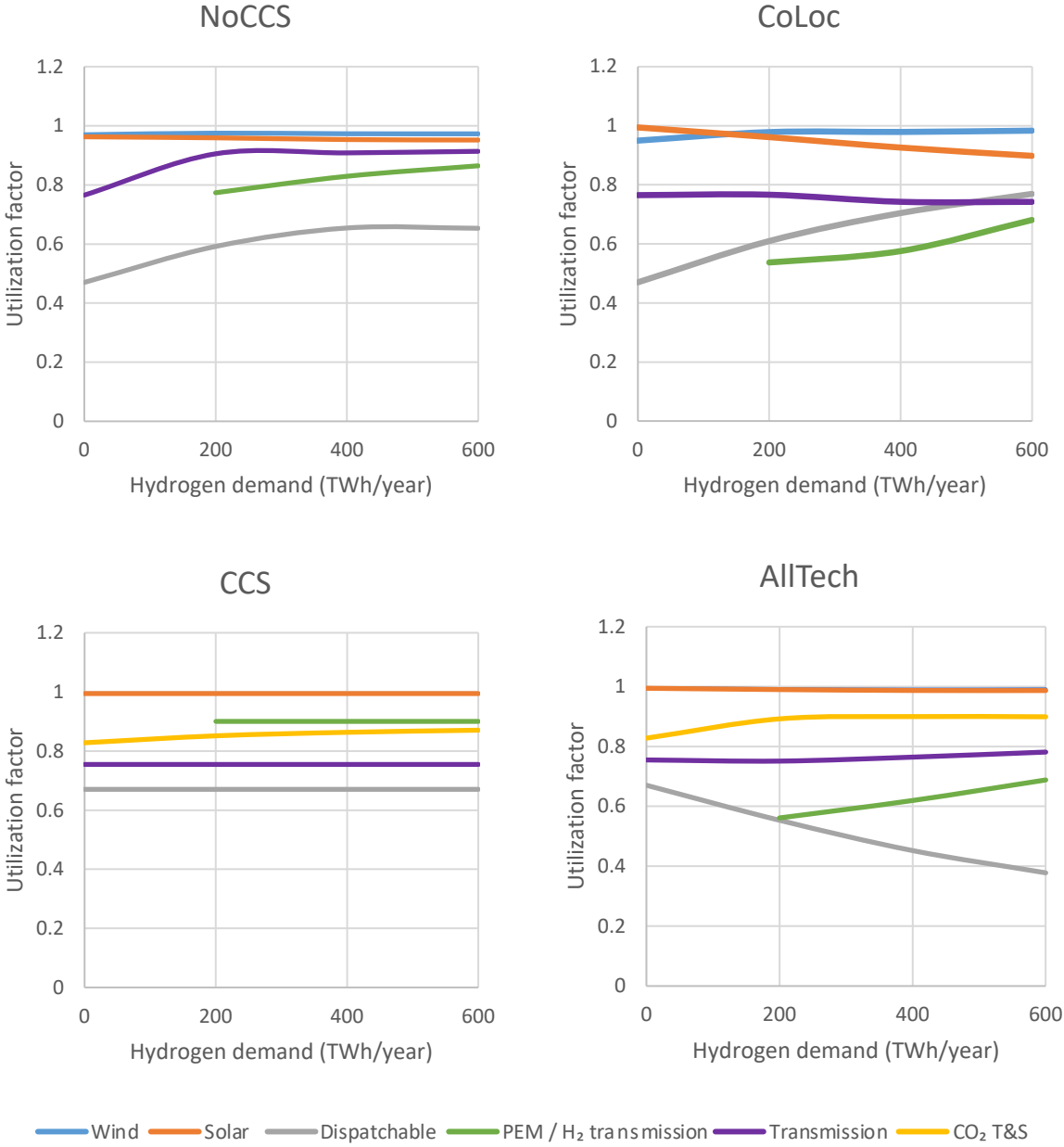


Figure 6: Capacity utilization factors of different parts of the energy system for the four different scenarios at different hydrogen demand levels.

Trends are different in the *CoLoc* scenario where large additional transmission network expansion to supply power to PEM facilities is avoided by co-locating PEM with wind. In this case, transmission network utilization shows a slight decline with hydrogen demand because of the absence of demand co-located PEM capacity to increase electricity demand in times of low system load and a decrease in battery deployment at high H₂ demand levels. The capacity factors of electrolysers and H₂ transmission lines are also lower as hydrogen production is more closely correlated with the co-located wind power. However, the 600 TWh/year hydrogen demand case shows a significant increase in PEM capacity factor. In this case, total annual hydrogen demand exceeds total electricity demand, reducing the

fraction of produced hydrogen that can be used to balance VRE to serve the fixed electricity demand profile. Hydrogen that cannot be used in such a balancing capacity is best produced at a higher capacity factor. For perspective, peak hydrogen storage in the *CoLoc* scenario is 2.6x greater than in the *NoCCS* scenario, making these costs more significant. The declining utilization factor of solar power is also noteworthy, illustrating that solar is not coupled to PEM for utilizing peak generation (Equation 28).

The *CCS* scenario shows almost no sensitivity to the hydrogen demand as hydrogen production is decoupled from electricity production. As shown, hydrogen is produced and transmitted at the maximum specified capacity factor of 90%. Dispatchable plants (mainly NGCC-CCS with peak load from unabated NGCC and OCGT plants) operate at a moderately high averaged capacity factor of 67% to balance the moderate levels of VRE indicated in Figure 3. The overall utilization of CO₂ T&S infrastructure increases with H₂ demand as SMR-CCS plants (used at their maximum 90% capacity factor) produce a larger fraction of the CO₂ for transport and storage.

In the *AllTech* scenario, the average capacity factor of dispatchable power plants declines and the utilization rate of hydrogen infrastructure increases with increased hydrogen demand. As a power plant, the capacity factor of GSR declines from 34% to 21% in the three cases with hydrogen demand, but the cost related to this low capacity factor is low as GSR is used in hydrogen production mode for the remainder of the time. Thus, as hydrogen demand increases, the larger GSR fleet increasingly transitions to hydrogen production, limiting the added costs related to intermittent hydrogen output. Increasing the utilization rate of hydrogen infrastructure as hydrogen demand increases is therefore a more economical option for GSR than integrating higher shares of VRE.

5.2 Effect of CO₂ prices

Figure 3 showed that CO₂ emissions remain significant at a CO₂ price of €100/ton, particularly in the green hydrogen scenarios. Deeper decarbonization will require further increases in the CO₂ price, as shown in Figure 7 (hydrogen demand set to 400 TWh/year). Trends in CO₂ emissions reduction differ between the green and blue hydrogen scenarios. In the *NoCCS* and *CoLoc* scenarios, rising CO₂ prices have a large effect due to the high share of unabated NGCC plants in these scenarios. The blue hydrogen scenarios have relatively high emissions at a CO₂ price of €50/ton because it is not yet economical to deploy CCS in the power sector at these CO₂ prices. However, an increase to €100/ton eliminates almost all unabated power plants, leading to sharp emissions reductions. The *AllTech* scenario features a gradual displacement of NGCC-CCS plants with GSR as the CO₂ price rises due to the low emissions intensity of GSR.

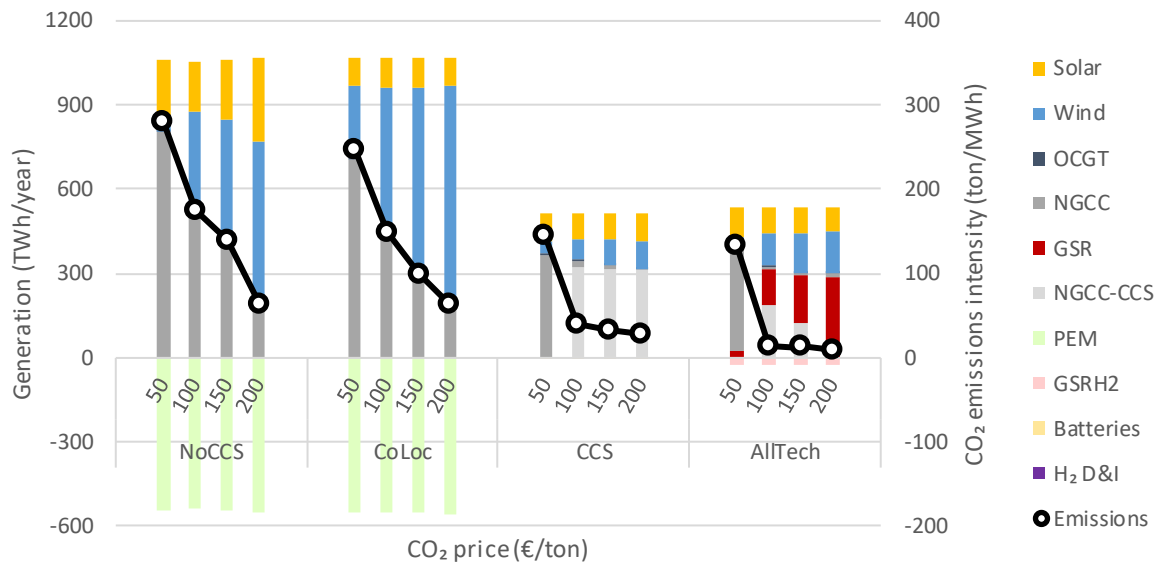


Figure 7: The optimal generation mix and associated CO₂ emissions in the four different scenarios at four different CO₂ price levels. Hydrogen demand is set to 400 TWh/year.

As shown in Figure 8, the sharp emissions reductions in the green hydrogen scenarios come at a considerable cost. In the *NoCCS* scenario with a €200/ton CO₂ price, it becomes economical to displace the majority of NGCC power production with VRE and use PEM as a balancing mechanism with a capacity factor of 50%, leading to a substantial increase in transmission system costs (the largest part of "other" costs in this case). The *CoLoc* scenario has a smoother trend where higher CO₂ prices gradually displace NGCC generation with wind power balanced by electrolysis operating at gradually reducing capacity factors. This reduces the utilization factors of both electrolysis and dispatchable plants to 39% at a €200/ton CO₂ price. The more intermittent hydrogen production from low capacity factor PEM also increases hydrogen transport and storage costs. Another interesting observation is that almost no hydrogen-fired power generation is deployed, even at high CO₂ prices, indicating the high cost of the power-to-gas-to-power pathway for balancing VRE. Only the *CoLoc* scenario deploys a small amount of H₂GT power production in the 150 and 200 €/ton CO₂ price scenarios, equivalent to 0.04% of total electricity generation.

It should be mentioned that the *CoLoc* scenario depends strongly on having cheap salt cavern storage co-located with good wind resources as well as access to a reliable hydrogen import supply. If salt cavern storage is unavailable at a CO₂ price of €200/ton (relying on more expensive tank storage), costs rise to the level of the *NoCCS* scenario, while hydrogen imports jump to 40% of demand. Higher hydrogen import prices strongly increase system costs in this case. As an example, salt cavern storage capacity is very unevenly distributed in Europe [42], so this limitation will be relevant to several regions.

Costs in the two blue hydrogen scenarios show only modest increases with CO₂ price and no hydrogen imports are required. At a CO₂ price of 200 €/ton, the annual total system cost of blue hydrogen scenarios is €29-41 billion lower than green hydrogen scenarios. For perspective, this is equivalent to about 1% of German GDP, close to the average annual economic growth rate since the turn of the century in real terms.

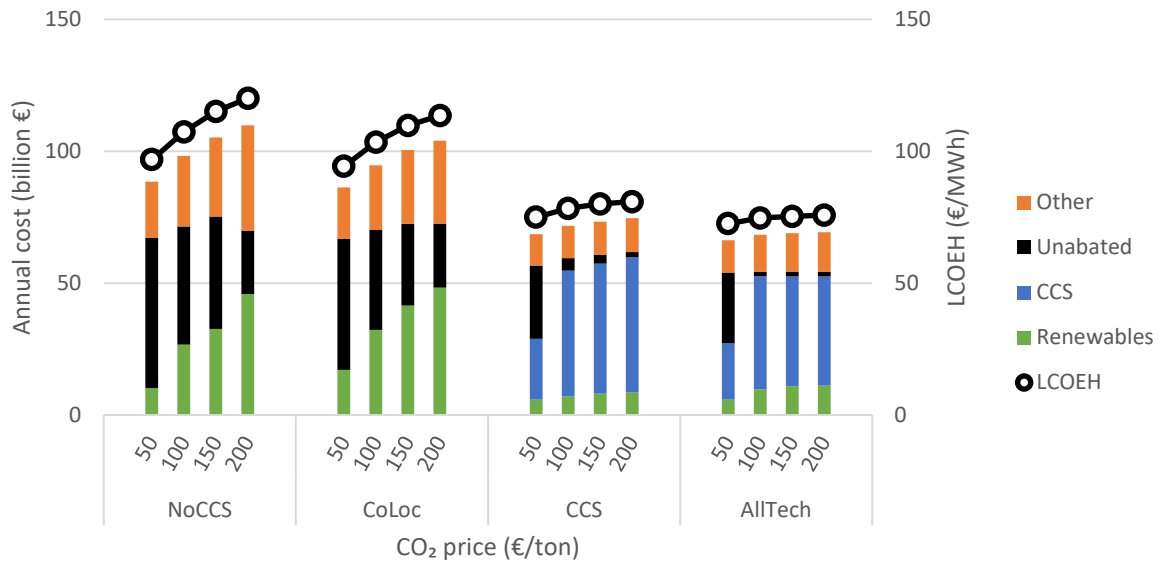


Figure 8: Costs involved in the four different scenarios at four different CO₂ price levels. Hydrogen demand is set to 400 TWh/year.

It should also be mentioned that, although incorporating higher shares of VRE in the blue hydrogen scenarios is not optimal, it is not exceedingly expensive either. As an example, Figure 9 shows the increase in LCOEH caused by decreasing the amount of natural gas available for consumption in the *AllTech* scenario. Natural gas consumption can be reduced from the optimal value of 991 TWh/year to 800 TWh/year at a negligible cost, mainly by displacing some GSR power production with VRE. Such a trade-off would be attractive for a natural gas importing region like Europe. However, further reductions become more costly as GSR hydrogen production must increasingly be replaced by PEM. If coal is allowed in the system, the VRE share remains relatively low as GSR is displaced by AUSC-CCS plants instead, significantly reducing costs relative to the cases without coal plotted in Figure 9.

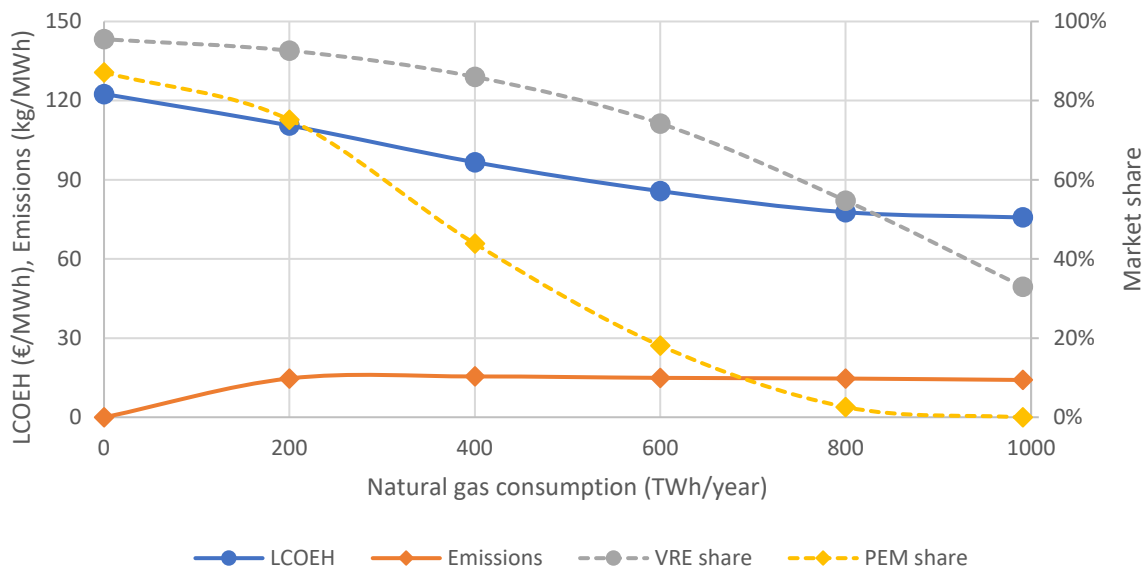


Figure 9: The cost of reducing natural gas consumption when no coal consumption is allowed at a CO₂ price of €200/ton.

5.3 Sensitivity to key model assumptions

This section presents the sensitivity to four sets of technology cost assumptions as well as the discount rate. The sensitivity ranges are specified in Table 5. Costs for electricity and gas grids are varied to a higher upper bound to account for the potentially large cost increases that could arise from public resistance to such infrastructure.

Table 5: Specifications of variable ranges in the sensitivity study relative to the values given in Table 1 and Table 2.

Short name	Description	Lower bound	Upper bound
Green	Wind, solar, PEM and battery costs	- 50%	+ 50%
Fossil	Coal and gas prices	- 50%	+ 50%
El grid	Transmission and added VRE transmission costs	- 50%	+ 100%
Gas grid	H ₂ and CO ₂ transmission and storage costs	- 50%	+ 100%
Discount	Discount rate	4%	10%

Results are summarized in Figure 10. As expected, the effect of changes to the costs of green technologies strongly affects the performance of the green hydrogen scenarios. The cost of the *CoLoc* scenario is particularly sensitive to these technology costs due to its high share of wind power and large PEM capacity used at a relatively low capacity factor. Although it is possible that green technology cost reductions continue to outperform expectations, it is worth mentioning that the *CoLoc* scenario deploys 356 GW of wind capacity at the lower cost bound. Wind power in Germany is currently experiencing considerable difficulties with permitting and public resistance at a capacity level of only 60 GW. Reaching the levels required by this scenario can therefore be expected to come at a sizable cost as wind power expansion moves further offshore and to increasingly remote regions.

Fossil fuel prices have a larger effect on the blue hydrogen scenarios, given their high consumption of natural gas. However, the lower bound in these scenarios is not realistic either, given that almost all power and hydrogen is generated from natural gas with almost no VRE deployment. At the upper price bound, most natural gas use in the power sector is displaced by coal with CCS and VRE. Fossil fuel prices also have a substantial effect on the green hydrogen scenarios, given their relatively high reliance on NGCC plants (Figure 3). High prices force PEM to operate at low capacity factors for balancing large VRE shares to displace expensive natural gas, leading to high transmission and storage system costs and a large decline in CO₂ emissions.

Electricity grid costs have the largest effect on the *NoCCS* scenario that is strongly constrained by the cost of transmitting power generated in windy and sunny regions to electrolyzers located close to demand centers. Co-location of wind and PEM capacity in the *CoLoc* scenario reduces this sensitivity. Grid expansion is another area facing considerable delays and public resistance in Germany at present, so higher costs related to project delays, administrative overheads and the need for underground transmission lines should be expected as the energy transition continues.

Hydrogen and CO₂ transmission and storage infrastructure is cheaper than electricity transmission and therefore show lower sensitivities in all scenarios. However, the *CoLoc* scenario is more sensitive to changes in these costs due to the need for a large hydrogen pipeline network to transmit hydrogen from a concentrated production region throughout the country. Public resistance could also impact the cost of this infrastructure, particularly if some accidents happen during this ambitious scale-up effort. It should also be mentioned that the highest hydrogen storage capacity deployed in this study

(the *CoLoc* scenario with optimistic green technology assumptions) amounts to 18 TWh, which is the energy equivalent of about 1000 Hiroshima-sized nuclear bombs. This opens the potential for black swan events similar to nuclear accidents turning public opinion against hydrogen. The blue hydrogen scenarios also show significant sensitivity because both H₂ and CO₂ T&S infrastructure affects these cases. However, the impact remains mild compared to most other sensitivities.

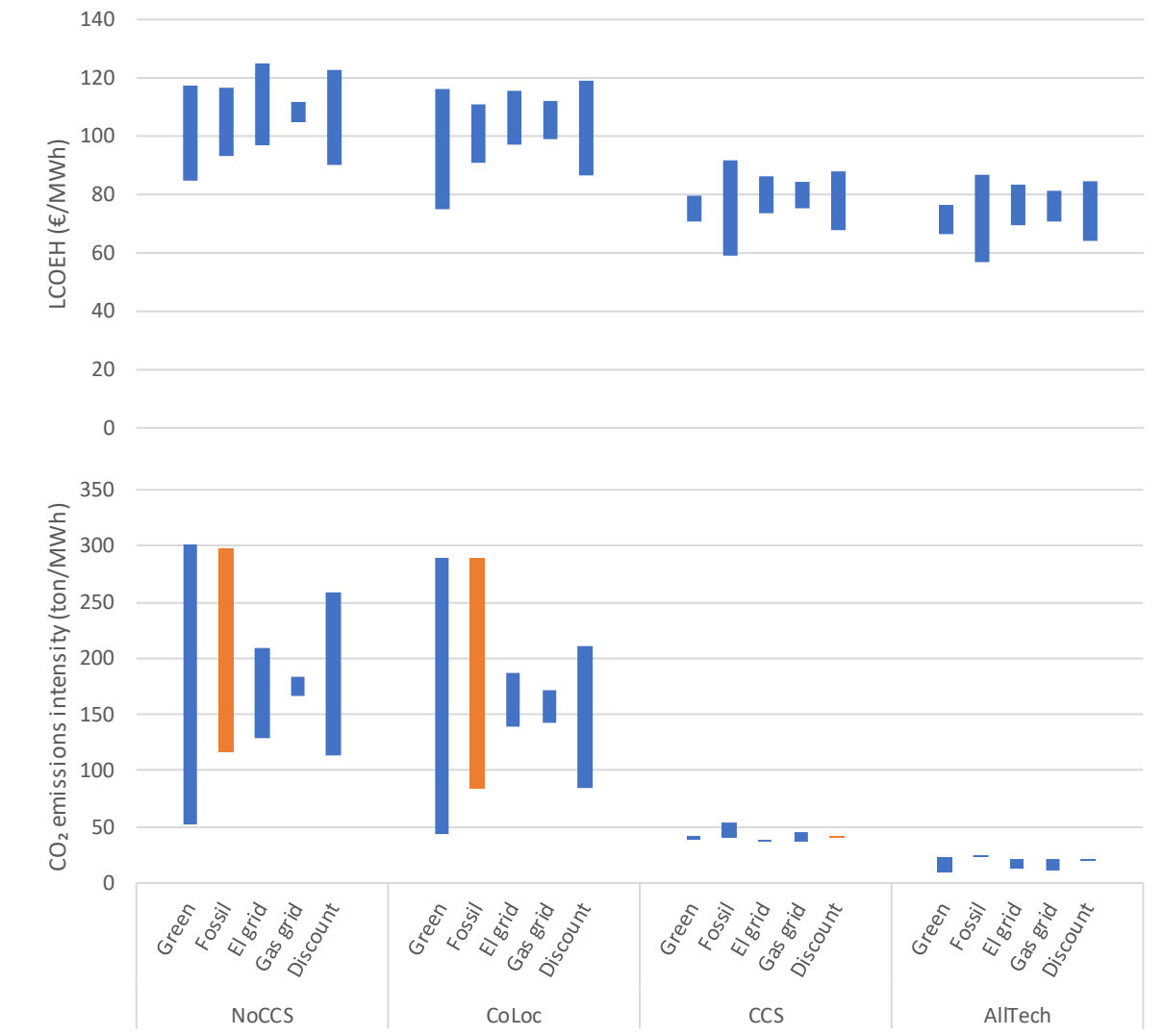


Figure 10: Sensitivity of the LCOEH and CO₂ emissions intensity to the perturbation specified in Table 5. Orange bars indicate cases where the lower bound is at the upper end of the bar and the upper bound at the lower end. The CO₂ price is set to €100/ton and the hydrogen demand to 400 TWh/year.

Finally, Figure 10 indicates a large sensitivity to the discount rate, particularly in the green hydrogen scenarios. In systems with low capacity utilization, a low discount rate is highly beneficial. Current weighted average capital costs for green technologies in developed nations are relatively low, but this is largely due to policies that shield investors against most market-related risk (e.g. value declines and curtailment as more wind and solar power is brought online, transmission bottlenecks occur, fossil fuel prices decline, extreme weather becomes more frequent, and low-carbon dispatchable plants with low running costs are commissioned). Such measures effectively shift risks from investors to ratepayers. Given that the global energy system must be rapidly and completely redesigned and rebuilt, risk and uncertainty in the energy sector have rarely been higher. The energy systems simulated in this study

are much more complex than the status quo and represent clearly disparate capital deployment pathways. This implies that system cost escalations, delays and accidents are likely, while any change in strategy along this multi-decade transition period will strongly devalue sunk investments. These factors suggest normalization to a high discount rate over time.

6 Summary and conclusions

Any system based on wind and solar energy will inevitably face reduced capital utilization rates: additional electricity must be supplied mainly during times of low wind and sun, energy must be consumed mainly during times of high wind and sun, or both. This study presented a model that captures the effects of such low capacity utilization in several optimized low-carbon energy system configurations for supplying clean electricity and hydrogen.

Four scenarios were investigated, two of which generate "green" hydrogen from wind and solar power and two also allowing for "blue" hydrogen from natural gas reforming with CCS. Each of these scenarios face different constraints from low capacity utilization when integrating higher shares of VRE. In each of them, the cost-optimal solution is shaped by the need to avoid idle capital:

- If green hydrogen is produced close to demand centers, electricity transmission costs have a substantial impact. Hence, the optimal energy mix utilized electrolyzers at high capacity factors to minimize these costs, mitigating the potential of electrolysis to balance VRE.
- This constraint is relieved if electrolysis is co-located with wind. However, low utilization of capital embodied in electrolyzers and the hydrogen transmission and storage infrastructure erodes the cost savings from avoiding electricity grid expansion. This scenario is also highly dependent on cheap salt cavern storage being available close to good wind or solar resources.
- When conventional CCS is deployed for blue hydrogen production, the optimal energy mix shows relatively low levels of VRE due to the cost of under-utilizing capital-intensive CCS power plants and CO₂ transport and storage infrastructure.
- A novel flexible CCS technology, GSR, could alleviate this constraint by operating continuously and alternating between power and hydrogen output depending on demand. However, limits arose from the low utilization rate of hydrogen transmission infrastructure and the need for greater hydrogen storage capacity for intermittently produced hydrogen.

For the green hydrogen scenarios, costs related to low capacity utilization intensify when striving for deep decarbonization through high CO₂ taxes as more variable wind and solar power must be integrated. Blue hydrogen scenarios are less sensitive due to less VRE deployment, reducing total system costs by the equivalent of about 1% of GDP relative to green hydrogen scenarios.

Further analysis revealed a high sensitivity to costs of VRE and the capital subject to low utilization rates in the green hydrogen scenarios. Grid costs strongly influenced the attractiveness of co-locating electrolyzers with demand, whereas wind-electrolysis co-location was influenced by electrolyzer and hydrogen transmission and storage costs. Optimistic technology cost reductions allow large overbuilds of VRE, electrolysis and transmission infrastructure, but such large capital expansion increases the likelihood of cost escalations from public resistance to wind turbines, transmission lines and hydrogen pipelines. The great complexity of these closely interconnected clean energy systems could lead to

further cost escalations. Blue hydrogen scenarios were generally simpler with sensitivity limited mainly to the natural gas price.

Low financing costs are key to the realization of these energy systems, particularly those relying on green hydrogen. High discount rates, reflecting the high risk and uncertainty inherent in a rapid and complete overhaul of the global energy system, strongly increase the cost of low capacity utilization. For this reason, an energy transition with high shares of VRE may well require perpetual policy support to eliminate uncertainty and shield investors from market risks to secure low financing costs, thus transferring most of the risk to the ratepayer.

In conclusion, the low capacity utilization inherent in energy systems with high shares of VRE substantially increases the total cost of such systems. Alternatives can be devised to increase utilization in one part of the system at the expense of another, but costs remain high in all cases. Such a whole-system perspective is important to take into consideration as the global energy transition continues.

7 Acknowledgement

We thank Jan Hendrik Cloete and Abdelghafour Zaabout for their helpful comments and discussions.

8 References

- [1] UNFCCC. Historic Paris Agreement on Climate Change. United Nations Framework Convention on Climate Change 2015.
- [2] IPCC. Global Warming of 1.5 °C. Intergovernmental Panel on Climate Change; 2018.
- [3] EU. A European Green Deal: Striving to be the first climate-neutral continent. European Union; 2019.
- [4] Parra D, Valverde L, Pino FJ, Patel MK. A review on the role, cost and value of hydrogen energy systems for deep decarbonisation. *Renewable and Sustainable Energy Reviews*. 2019;101:279-94.
- [5] EU. Hydrogen Roadmap Europe: A sustainable pathway for the European energy transition. European Union; 2019.
- [6] US. Road Map to a US Hydrogen Economy: Reducing emissions and driving growth across the nation. Fuel Cell & Hydrogen Energy Association; 2019.
- [7] Gummer J, King J, Chater N, Heaton R, Johnson P, Quéré CL, et al. Hydrogen in a low-carbon economy. Committee on Climate Change; 2018.
- [8] Bruce S, Temminghoff M, Hayward J, Schmidt E, Munnings C, Palfreyman D, et al. National Hydrogen Roadmap: Pathways to an economically sustainable hydrogen industry in Australia. CSIRO; 2018.
- [9] IRENA. Hydrogen: A renewable energy perspective. International Renewable Energy Agency; 2019.
- [10] IEA. The future of hydrogen: Seizing today's opportunities. International Energy Agency; 2019.
- [11] Agora Verkehrswende and Agora Energiewende. The Future Cost of Electricity-Based Synthetic Fuels. 2018.
- [12] Reuß M, Grube T, Robinius M, Preuster P, Wasserscheid P, Stolten D. Seasonal storage and alternative carriers: A flexible hydrogen supply chain model. *Applied Energy*. 2017;200:290-302.
- [13] Emonts B, Reuß M, Stenzel P, Welder L, Knicker F, Grube T, et al. Flexible sector coupling with hydrogen: A climate-friendly fuel supply for road transport. *International Journal of Hydrogen Energy*. 2019;44(26):12918-30.
- [14] EIA. Gasoline explained: Factors affecting gasoline prices. In: Administration USEI, editor. 2019.
- [15] Samsatli S, Staffell I, Samsatli NJ. Optimal design and operation of integrated wind-hydrogen-electricity networks for decarbonising the domestic transport sector in Great Britain. *International Journal of Hydrogen Energy*. 2016;41(1):447-75.
- [16] Welder L, Ryberg DS, Kotzur L, Grube T, Robinius M, Stolten D. Spatio-temporal optimization of a future energy system for power-to-hydrogen applications in Germany. *Energy*. 2018;158:1130-49.

- [17] Qadrdan M, Abeysekera M, Chaudry M, Wu J, Jenkins N. Role of power-to-gas in an integrated gas and electricity system in Great Britain. *International Journal of Hydrogen Energy*. 2015;40(17):5763-75.
- [18] de Boer HS, Grond L, Moll H, Benders R. The application of power-to-gas, pumped hydro storage and compressed air energy storage in an electricity system at different wind power penetration levels. *Energy*. 2014;72:360-70.
- [19] Brown T, Schlachtberger D, Kies A, Schramm S, Greiner M. Synergies of sector coupling and transmission reinforcement in a cost-optimised, highly renewable European energy system. *Energy*. 2018;160:720-39.
- [20] Spallina V, Pandolfo D, Battistella A, Romano MC, Van Sint Annaland M, Gallucci F. Techno-economic assessment of membrane assisted fluidized bed reactors for pure H₂ production with CO₂ capture. *Energy Conversion and Management*. 2016;120:257-73.
- [21] Cloete S, Khan MN, Amini S. Economic assessment of membrane-assisted autothermal reforming for cost effective hydrogen production with CO₂ capture. *International Journal of Hydrogen Energy*. 2019;44(7):3492-510.
- [22] Cloete S, Hirth L. Flexible power and hydrogen production: Finding synergy between CCS and variable renewables. *Energy*. 2020;192:116671.
- [23] Wassie SA, Gallucci F, Zaabout A, Cloete S, Amini S, van Sint Annaland M. Hydrogen production with integrated CO₂ capture in a novel gas switching reforming reactor: Proof-of-concept. *International Journal of Hydrogen Energy*. 2017;42(21):14367-79.
- [24] Szima S, Nazir SM, Cloete S, Amini S, Fogarasi S, Cormos A-M, et al. Gas switching reforming for flexible power and hydrogen production to balance variable renewables. *Renewable and Sustainable Energy Reviews*. 2019;110:207-19.
- [25] Robinius M, Otto A, Syranidis K, Ryberg DS, Heuser P, Welder L, et al. Linking the Power and Transport Sectors—Part 2: Modelling a Sector Coupling Scenario for Germany. 2017;10(7):957.
- [26] Neon. Open Power System Database. 2019.
- [27] IEA. World Energy Outlook. International Energy Agency; 2019.
- [28] NREL. Annual technology baseline. National Renewable Energy Laboratory. <https://atb.nrel.gov/electricity/2018/index.html?t=cg> [Accessed: 24.10.2019]; 2018.
- [29] Walker I, Madden B, Tahir F. Hydrogen supply chain evidence base. Elemental Energy; 2018.
- [30] IEA. Projected Costs of Generating Electricity. International Energy Agency and Nuclear Energy Agency; 2015.
- [31] Franco F, Anantharaman R, Bolland O, Booth N, van Dorst E, Ekstrom C, et al. European Best Practice Guidelines for CO₂ Capture Technologies. CESAR project: European Seventh Framework Programme 2011.
- [32] IEAGHG. The costs of CO₂ storage: Post-demonstration CCS in the EU. European technology platform for zero emission fossil fuel power plants; 2011.
- [33] IEAGHG. The costs of CO₂ transport: Post-demonstration CCS in the EU. European technology platform for zero emission fossil fuel power plants; 2011.
- [34] Thalman E, Wehrmann B. What German households pay for power. *Clean Energy Wire*. <https://www.cleanenergywire.org/factsheets/power-grid-fees-unfair-and-opaque> [Accessed: 09.04.2020]; 2020.
- [35] TenneT. German Regulation. <https://www.tennet.eu/e-insights/regulation/german-regulation/> [Accessed: 09.04.2020]; 2020.
- [36] Gorman W, Mills A, Wiser R. Improving estimates of transmission capital costs for utility-scale wind and solar projects to inform renewable energy policy. *Energy Policy*. 2019;135:110994.
- [37] Caglayan D, Weber N, Heinrichs HU, Linßen J, Robinius M, Kukla PA, et al. Technical Potential of Salt Caverns for Hydrogen Storage in Europe. Preprints 2019.
- [38] Ahluwalia RK, Papadias DD, Peng J-K, Roh HS. System Level Analysis of Hydrogen Storage Options. In: Laboratory AN, editor.: US Department of Energy; 2019.
- [39] Siemens. Siemens HL: The bridge to 65%+ efficiency. *Modern Power Systems*; 2018.

- [40] Kvamsdal HM, Romano MC, van der Ham L, Bonalumi D, van Os P, Goetheer E. Energetic evaluation of a power plant integrated with a piperazine-based CO₂ capture process. *International Journal of Greenhouse Gas Control*. 2014;28:343-55.
- [41] Rubin ES, Davison JE, Herzog HJ. The cost of CO₂ capture and storage. *International Journal of Greenhouse Gas Control*. 2015;40:378-400.
- [42] Caglayan DG, Weber N, Heinrichs HU, Linßen J, Robinius M, Kukla PA, et al. Technical potential of salt caverns for hydrogen storage in Europe. *International Journal of Hydrogen Energy*. 2020;45(11):6793-805.